Figure 7-7: Photo of the modelled Transport&Logistics@Sea hub with cranes, container stacks and vessel

Figure 7-8: Photo of the modelled Transport&Logistics@Sea hub with the buildings and tower of the control centre

8. Summary, Conclusions and Recommendations

Based on the results presented in this report, following summary, conclusions and recommendations seem to be justified:

- The concept of an island consisting of several squared modules in general behaves as expected.
- There is a good agreement between the static load tests and the theoretical offset-force curve. The static load tests confirmed a proper modelling and installation of the mooring system in the test-setup.
- The decay tests showed a beating pattern with amplifications of the signal, typical for multiple modes interacting. The natural frequency of surge, sway and yaw lay between 155s and 180s.
- In currents, the island was stable.
- The measured motions in surge, sway and yaw are characterized by the low frequent content. Almost no wave frequent or high frequent horizontal motions were measured.
- The MPM pitch angle of each test has been derived for all modules with a measuring target. The front rows shelter the leeward ones, helping to decrease the pitch due to wave diffraction on keel. For the 1, 10 and 100 years sea states, however, the modules at the rear of the island show larger pitch amplitudes, than the modules at the front. The reason could be that the modules installed at the stern were smaller (45m x 45m) than at the front (95m x 95m) and therefore had a larger pitch response in the tested storm sea states (see also [1]). Furthermore, the modules at the rear row were not moored and not surrounded at all sides by other modules so that they were less restricted to pitch.
- During the tests, there was no tension measured in the fenders, which means that the pretension of the cable wires was sufficient to maintain compression in the fenders in tested waves and current.
- Compression and vertical shear forces of the clustered fender setup in the tank tests need to be compared with the design of the Graz-connector and its dimensioning. As expected, the connectors showed the highest vertical shear for waves approaching under an angle (to 225 degrees), when the wave propagation is oblique to the fenders due to the square geometry of the modules.
- The measured mooring line tensions are all below the MBL, with a safety factor slightly higher than 2. In general, there is no significant difference between the tests with and without current, except for the 100 year case where the mooring line got fully tensioned in the test with current. Therefore, it is recommended to increase the mooring radius and line length for similar island layouts and installation sites with those conditions.
- In storm sea states, significant amount of green water on deck of the waveward modules has been observed. Whereas water on deck of the WECs is unproblematic, water on deck of the standard modules needs to be prevented in any case. Stacked containers at the waveward side will not be sufficient so that the installation of bulwarks at the critical locations is proposed in this report. This solution seems to be economically and technically feasible. It should be studied how large the impact loads at the bulwarks will be and how the loads and amount of green water change when the WECs are realistically damped and show the correct pitch amplitudes.
- A harbor basin with the entry facing away from the waves seems to be a good shelter if vessels shall be moored to the island. Although no wave height measurements were performed inside the harbour during the tank tests, from photo and video it can be seen that the wave height there is significantly reduced.
- With the chosen side-by-side mooring, the standard deviation of translational motions of the vessel goes up to about 1.5m in x direction. Rotations show a standard deviation of up to 0.55 degrees in roll. The values should be compared with the motions appearing when the vessel is connected by the vacuum mooring system, developed in Task 9.5 [9].

In future studies, based on the tank test results, design adaptions of the Space@Sea island and its subsystems should be made. Besides the already mentioned ones above, it should be discussed, whether it is possible to only use the 95m x 95m- modules or similar ones. By that, the natural pitch response would be shifted away from energetic sea states and critical pitch amplitudes avoided. In any case, also the modules at the rear should be moored at the outer edge of the island.

Besides further checks and development work of the island's subsystems (connectors, mooring for different installation sites, etc.), the numerical model should be validated with the results of the tank tests. With further numerical analyses of exemplary islands, design recommendations regarding favourable island layouts could be developed. For example, it could then be indicated, where the different use-cases are to be placed on the island, depending on their limiting criteria.

And last but not least, the tank test results and learnings about motions and loads of the Space@Sea island should be input for economic analyses and optimisations in order to eventually gain a technically and economically feasible concept for floating multi-purpose-islands.

References

[1] C. Hüsken, W. Otto (MARIN); J. Schay (NEMOS); G. Assbrock (DST); A. Cobzaru (ICE); D. Kirkwood (Blue21), "Integrated Design and Realisation of Integrated Model - Deliverable 10.3," Space@Sea Project, Wageningen, 2020.

[2] J. C. (UDE), "Limiting Criteria - Deliverable 4.5," Space@Sea Project, Duisburg, 2020.

[3] M. Flikkema; K. Czapiewska; B. Holtmann; J. Peckolt; C. Thill; J. Kymmell; M. Abdel-Maksoud; C. v.d. Nat; U. Ritschel; F. Adam; R. Jak; O. El Moctar; K. Ellermann; A. Stam; C. Landa; H. Mortensen; F. Verschraegen, "Proposal: Space@Sea (Nr. 774253)," 2017.

[4] Oil Companies International Marine Forum (OCIMF), Prediction of Wind and Current Loads on VLCCs, 2nd edition ed., 1994.

[5] I. Drummen, W. Otto (MARIN); C. Thill, M. Hassan (TU Delft); C. Nichols (Bluewater), "Basic Design Report - Deliverable 4.2," Space@Sea Project, Wageningen, 2018.

[6] M. Breuls (Mocean); S. Blumer (ICE); N. Jacob; B. Blümel (Tu Graz), "Detail Design Report - Deliverable 4.4," Space@Sea Project, 2020.

[7] C. Hüsken, J. Lucas, J. Peckolt (NEMOS); G. Assbrock, J. Ley (DST); G. Olbert, M. Engels (TUHH), "Method to harvest energy from relative motion - Deliverable 6.1," Space@Sea Project, Duisburg, 2019.

[8] T. van Rossum (Bluewater); W. Otto (MARIN), "Mooring System Design - Deliverable 3.3," Space@Sea, 2020.

[9] Souravlias, D., Duinkerken, M.B., Negenborg, R.R. (TU Delft); Morshuis, S. (MOCEAN); Assbrock, G., Ley, J. (DST), "Operational process coordination strategy - Deliverable 9.4," Space@Sea Project, 2019.

[10] C. Hüsken (NEMOS); M. Flikkema (MARIN), "Factsheet - Frequently Updated Memorandum on Deliverable 10.1," Space@Sea Project, 2019.

TABLES

TABLE 1 OVERVIEW OF CURRENT CALIBRATION WITHOUT MODEL

Stationary measurements

MARIN Test No. 30381_02OB_01_	Description	Specified speed [m/s]	Current direction [deg]	Measured speed [m/s]	Turbulence [%]	Depth [m]
010_002_01	Current at CL position	1.000	180	1.018	8.5	12.0
010_003_01	Current at REF position	1.000	180	1.020	5.9	30.0

TABLE 2 OVERVIEW OF CALIBRATED IRREGULAR WAVES WITHOUT MODEL

MARIN Test No. 30381_02OB_02_	Description	Time	Irregular Sea Characteristics JONSWAP Type Spectrum				Current		Realised		Error	
			Hs	Tp	Dir.	γ	Vc	Dir	Hs	Tp	Hs	Tp
		[hrs]	[m]	[s]	[deg]	[-]	[m/s]	[deg]	[m]	[s]	[%]	[%]
without current												
003_003_01	Operational 180	½ + 3	2.00	5.50	180	3.30	-	-	1.942	5.512	-2.9	0.2
004_003_01	Operational 210			6.50	210				1.838	6.545	-8.1	0.7
005_003_01	Operational 225			7.50	225				1.797	7.480	-10.2	-0.3
006_003_01	1yr 180		3.00	6.50	180				2.970	6.412	-1.0	-1.4
007_003_01	1yr 210			7.50	210				2.879	7.480	-4.0	-0.3
008_002_01	1yr 225			8.00	225				2.900	8.056	-3.3	0.7
009_003_01	10yr 180		5.00	8.00	180				4.978	8.056	-0.4	0.7
010_003_01	10yr 210				210				4.816	8.056	-3.7	0.7
011_002_01	100yr 180		5.90	10.50	180				5.859	10.472	-0.7	-0.3
with current												
012_003_01	Operational 180 CUR	½ + 3	2.00	5.50	180	3.30	1.0	180	1.891	5.417	-5.5	-1.5
013_004_01	Operational 210 CUR			6.50	210				1.789	6.412	-10.6	-1.4
015_003_01	Operational 225 CUR			7.50	225				1.877	7.480	-6.2	-0.3
021_003_01	1yr 180 CUR		3.00	6.50	180				2.934	6.412	-2.2	-1.4
016_003_01	1yr 210 CUR			7.50	210				2.942	7.480	-1.9	-0.3
018_002_01	1yr 225 CUR			8.00	225				2.888	8.056	-3.7	0.7
022_003_01	10yr 180 CUR		5.00	8.00	180				4.938	8.056	-1.2	0.7
020_003_01	10yr 210 CUR				210				4.945	8.056	-1.1	0.7
023_002_01	100yr 180 CUR		5.90	10.50	180				5.865	10.472	-0.6	-0.3

TABLE 3 LOCATION OF TARGETS

Location	X w.r.t Origin (K8)	Y w.r.t. Origin (K8)	Z w.r.t. Keel
	[m]	[m]	[m]
Target_L1	259.11	234.12	20.00
Target_L2	259.11	169.65	20.00
Target_L4	215.81	-87.46	20.00
Target_L7	194.64	234.12	20.00
Target_L8	194.64	169.65	20.00
Target_L10	159.15	-105.94	20.00
Target_L11	159.15	-165.72	20.00
Target_L12	159.15	-230.19	20.00
Target_L15	-40.77	234.12	20.00
Target_L16	-40.77	134.16	20.00
Target_S4	315.60	127.77	13.00
Target_S13	265.50	290.49	13.00
Target_S14	234.12	290.49	13.00
Target_S15	194.64	290.49	13.00
Target_M1	94.68	-230.19	20.00
Target_M2	94.68	-280.17	20.00
Target_M12	-174.42	-159.33	20.00
Target_M13	-184.32	-190.71	20.00
Target_M14	-184.32	-240.69	20.00
Target_M15	-184.32	-294.27	20.00
Target_M19	-215.70	-159.33	20.00
Target_M20	-215.70	-190.71	20.00
Target_M21	-215.70	-240.69	20.00
Target_M22	-215.70	-280.17	20.00
Target_M25	-265.68	-159.33	20.00
Target_M26	-265.68	-190.71	20.00
Target_M27	-265.68	-240.69	20.00
Target_M28	-265.68	-280.17	20.00
Target_M31	-307.02	-159.33	20.00
Target_M32	-305.16	-190.71	20.00
Target_M33	-305.16	-240.69	20.00
Target_container	-53.09	104.76	46.98

TABLE 4 LOCATION OF SIX COMPONENT FRAMES

Location	X w.r.t Origin (K8)	Y w.r.t. Origin (K8)	Z w.r.t. Keel
	[m]	[m]	[m]
Frame L1_1	211.62	274.14	8.40
Frame L1_2	211.62	244.14	8.40
Frame L1_3	211.62	224.16	8.40
Frame L1_4	211.62	194.16	8.40
Frame L2_1	299.10	181.68	8.40
Frame L2_2	219.12	181.68	8.40
Frame L121	111.66	-225.72	8.40
Frame L122	111.66	-255.72	8.40
Frame L123	111.66	-275.70	8.40
Frame L124	111.66	-305.70	8.40

TABLE 5 LOCATION OF MOORING LINES

Location	Fairlead location			Anchor location		
	X w.r.t Origin (K8)	Y w.r.t. Origin (K8)	Z w.r.t. Keel	X w.r.t Origin (K8)	Y w.r.t. Origin (K8)	Z w.r.t. Keel
	[m]	[m]	[m]	[m]	[m]	[m]
Mooring Line 1	306.60	259.14	0.00	876.10	259.14	-92.00
Mooring Line 2	306.60	209.16	0.00	876.10	209.16	-92.00
Mooring Line 3	306.60	159.18	0.00	876.10	159.18	-92.00
Mooring Line 4	306.60	109.20	0.00	876.10	109.20	-92.00
Mooring Line 5	306.60	59.22	0.00	876.10	59.22	-92.00
Mooring Line 6	306.60	9.24	0.00	876.10	9.24	-92.00
Mooring Line 7	306.60	-40.80	0.00	876.10	-40.80	-92.00
Mooring Line 8	306.60	-90.78	0.00	876.10	-90.78	-92.00
Mooring Line 9	306.60	-140.76	0.00	876.10	-140.76	-92.00
Mooring Line 10	306.60	-190.74	0.00	876.10	-190.74	-92.00
Mooring Line 11	306.60	-240.72	0.00	876.10	-240.72	-92.00
Mooring Line 12	306.60	-290.70	0.00	876.10	-290.70	-92.00
Mooring Line 13	284.10	281.64	0.00	284.10	851.14	-92.00
Mooring Line 14	234.12	281.64	0.00	234.12	851.14	-92.00
Mooring Line 15	184.14	281.64	0.00	184.14	851.14	-92.00
Mooring Line 16	134.16	281.64	0.00	134.16	851.14	-92.00
Mooring Line 17	84.18	281.64	0.00	84.18	851.14	-92.00
Mooring Line 18	34.20	281.64	0.00	34.20	851.14	-92.00
Mooring Line 19	-15.78	281.64	0.00	-15.78	851.14	-92.00
Mooring Line 20	-65.76	281.64	0.00	-65.76	851.14	-92.00
Mooring Line 21	-165.72	281.64	0.00	-165.72	851.14	-92.00
Mooring Line 22	-115.74	281.64	0.00	-115.74	851.14	-92.00

TABLE 6 LOCATION OF SIDE BY SIDE LINES

Location	X w.r.t Origin (K8)	Y w.r.t. Origin (K8)	Z w.r.t. Keel
	[m]	[m]	[m]
SBS L1	211.62	274.14	11.88
SBS L2	211.62	244.14	11.88
SBS L3	211.62	224.16	11.88
SBS L4	211.62	194.16	11.88
SBS L5	299.10	181.68	11.88
SBS L6	269.10	181.68	11.88
SBS L7	249.12	181.68	11.88
SBS L8	219.12	181.68	11.88
SBS L9	111.66	-225.72	11.88
SBS L10	111.66	-255.72	11.88
SBS L11	111.66	-275.70	11.88
SBS L12	111.66	-305.70	11.88

TABLE 7 LOCATION OF COG OF THE ISLANDS

Location	X w.r.t Origin (K8)	Y w.r.t. Origin (K8)	Z w.r.t. Keel
	[m]	[m]	[m]
Target_L1	259.11	234.12	20.00
Target_L2	259.11	169.65	20.00
Target_L4	215.81	-87.46	20.00
Target_L7	194.64	234.12	20.00
Target_L8	194.64	169.65	20.00
Target_L10	159.15	-105.94	20.00
Target_L11	159.15	-165.72	20.00
Target_L12	159.15	-230.19	20.00
Target_L15	-40.77	234.12	20.00
Target_L16	-40.77	134.16	20.00
Target_S4	315.60	127.77	13.00
Target_S13	265.50	290.49	13.00
Target_S14	234.12	290.49	13.00
Target_S15	194.64	290.49	13.00
Target_M1	94.68	-230.19	20.00
Target_M2	94.68	-280.17	20.00
Target_M12	-174.42	-159.33	20.00
Target_M13	-184.32	-190.71	20.00
Target_M14	-184.32	-240.69	20.00
Target_M15	-184.32	-294.27	20.00
Target_M19	-215.70	-159.33	20.00
Target_M20	-215.70	-190.71	20.00
Target_M21	-215.70	-240.69	20.00
Target_M22	-215.70	-280.17	20.00
Target_M25	-265.68	-159.33	20.00
Target_M26	-265.68	-190.71	20.00
Target_M27	-265.68	-240.69	20.00
Target_M28	-265.68	-280.17	20.00
Target_M31	-307.02	-159.33	20.00
Target_M32	-305.16	-190.71	20.00
Target_M33	-305.16	-240.69	20.00
Target_container	-53.09	104.76	46.98

TABLE 8 DESIGNATION, NOTATION, SIGN CONVENTION AND MEASURING DEVICE OF MEASURED QUANTITIES (I/IX)

Designation:	Notation:	Positive for:	Measured by:
WAVE ELEVATIONS AT REFERENCE POINTS:			
For locations see figure	WAVE_180 WAVE_210 WAVE_225 WAVE_CL	Wave crest	Resistance type wave probes
WAVE FLAP ANGLE:			
From 180 degrees From 270 degrees	STROKE_W STROKE_Z	Into the basin	-
TENSION IN SPREAD MOORING LINES:			
22 Spread mooring lines	F_MOOR_01 to F_MOOR_22	Tension	Ring shaped force transducers
TENSION IN SIDE-BY-SIDE LINES:			
12 Side-by-side lines	F_SBS_01 to F_SBS_12	Tension	Ring shaped force transducers

TABLE 9 DESIGNATION, NOTATION, SIGN CONVENTION AND MEASURING DEVICE OF MEASURED QUANTITIES (II/IX)

Designation:	Notation:	Positive for:	Measured by:
FORCES MEASURED IN 6-COMPONENT FORCE FRAMES L1-1 to L1-4 (NUMBERED FROM PORT SIDE TO STARBOARD):			
Six component frame L1-1:		**Force applied:**	6 component force frames
Longitudinal force (S1)	FXCLU_L1-1	L1 Forward	
Longitudinal force (S3)	FXPSL_L1-1	L1 Forward	
Longitudinal force (S2)	FXSBL_L1-1	L1 Forward	
Tranverse force (S4)	FY_L1-1	L1 To portside	
Vertical force (S6)	FZ_PS_L1-1	L1 Upward	
Vertical force (S5)	FZ_SB_L1-1	L1 Upward	
Six component frame L1-2:		**Force applied:**	
Longitudinal force (S1)	FXCLU_L1-2	L1 Forward	
Longitudinal force (S3)	FXPSL_L1-2	L1 Forward	
Longitudinal force (S2)	FXSBL_L1-2	L1 Forward	
Tranverse force (S4)	FY_L1-2	L1 To portside	
Vertical force (S6)	FZ_PS_L1-2	L1 Upward	
Vertical force (S5)	FZ_SB_L1-2	L1 Upward	
Six component frame L1-3:		**Force applied:**	
Longitudinal force (S1)	FXCLU_L1-3	L1 Forward	
Longitudinal force (S3)	FXPSL_L1-3	L1 Forward	
Longitudinal force (S2)	FXSBL_L1-3	L1 Forward	
Tranverse force (S4)	FY_L1-3	L1 To portside	
Vertical force (S6)	FZ_PS_L1-3	L1 Upward	
Vertical force (S5)	FZ_SB_L1-3	L1 Upward	
Six component frame L1-4:		**Force applied:**	
Longitudinal force (S1)	FXCLU_L1-4	L1 Forward	
Longitudinal force (S3)	FXPSL_L1-4	L1 Forward	
Longitudinal force (S2)	FXSBL_L1-4	L1 Forward	
Tranverse force (S4)	FY_L1-4	L1 To portside	
Vertical force (S6)	FZ_PS_L1-4	L1 Upward	
Vertical force (S5)	FZ_SB_L1-4	L1 Upward	
FORCES MEASURED IN 6-COMPONENT FORCE FRAMES L2-1 to L2-2 (NUMBERED FROM FORE TO AFT):			
Six component frame L2-1:		**Force applied:**	6 component force frames
Longitudinal force (S4)	FX_L2-1	L1 Forward	
Tranverse force (S1)	FYCLU_L2-1	L1 Forward	
Tranverse force (S3)	FY_FL_L2-1	L1 Forward	
Tranverse force (S2)	FY_AL_L2-1	L1 To portside	
Vertical force (S6)	FZ_F_L2-1	L1 Upward	
Vertical force (S5)	FZ_A_L2-1	L1 Upward	
Six component frame L2-2:		**Force applied:**	
Longitudinal force (S4)	FX_L2-2	L1 Forward	
Tranverse force (S1)	FYCLU_L2-2	L1 Forward	
Tranverse force (S3)	FY_FL_L2-2	L1 Forward	
Tranverse force (S2)	FY_AL_L2-2	L1 To portside	
Vertical force (S6)	FZ_F_L2-2	L1 Upward	
Vertical force (S5)	FZ_A_L2-2	L1 Upward	

TABLE 10 DESIGNATION, NOTATION, SIGN CONVENTION AND MEASURING DEVICE OF MEASURED QUANTITIES (III/IX)

Designation:	Notation:	Positive for:	Measured by:
FORCES MEASURED IN 6-COMPONENT FORCE FRAMES L12-1 to L12-4 (NUMBERED FROM PORT SIDE TO STARBOARD):			
Six component frame L121:		**Force applied:**	6 component force frames
Longitudinal force (S1)	FXCLU_L121	L12 Forward	
Longitudinal force (S3)	FXPSL_L121	L12 Forward	
Longitudinal force (S2)	FXSBL_L121	L12 Forward	
Tranverse force (S4)	FY_L121	L12 To portside	
Vertical force (S6)	FZ_PS_L121	L12 Upward	
Vertical force (S5)	FZ_SB_L121	L12 Upward	
Six component frame L122:		**Force applied:**	
Longitudinal force (S1)	FXCLU_L122	L12 Forward	
Longitudinal force (S3)	FXPSL_L122	L12 Forward	
Longitudinal force (S2)	FXSBL_L122	L12 Forward	
Tranverse force (S4)	FY_L122	L12 To portside	
Vertical force (S6)	FZ_PS_L122	L12 Upward	
Vertical force (S5)	FZ_SB_L122	L12 Upward	
Six component frame L123:		**Force applied:**	
Longitudinal force (S1)	FXCLU_L123	L12 Forward	
Longitudinal force (S3)	FXPSL_L123	L12 Forward	
Longitudinal force (S2)	FXSBL_L123	L12 Forward	
Tranverse force (S4)	FY_L123	L12 To portside	
Vertical force (S6)	FZ_PS_L123	L12 Upward	
Vertical force (S5)	FZ_SB_L123	L12 Upward	
Six component frame L124:		**Force applied:**	
Longitudinal force (S1)	FXCLU_L124	L12 Forward	
Longitudinal force (S3)	FXPSL_L124	L12 Forward	
Longitudinal force (S2)	FXSBL_L124	L12 Forward	
Tranverse force (S4)	FY_L124	L12 To portside	
Vertical force (S6)	FZ_PS_L124	L12 Upward	
Vertical force (S5)	FZ_SB_L124	L12 Upward	

TABLE 11 DESIGNATION, NOTATION, SIGN CONVENTION AND MEASURING DEVICE OF MEASURED QUANTITIES (IV/IX)

Designation:	Notation:	Positive for:	Measured by:
MOTIONS OF DRIVING ISLAND L1 AT TARGET POSITION:			
Translations:		**Island moving:**	NDI optical measuring system
Longitudinal motion	XT_L1	Forward	
Transverse motion	YT_L1	To portside	
Vertical motion	ZT_L1	Upward	
Rotations:		**Island moving:**	
Around longitudinal axis	R_L1	Starboard down	
Around transverse axis	P_L1	Bow down	
Around vertical axis	Y_L1	Bow to portside	
MOTIONS OF DRIVING ISLAND L2 AT TARGET POSITION:			
Translations:		**Island moving:**	NDI optical measuring system
Longitudinal motion	XT_L2	Forward	
Transverse motion	YT_L2	To portside	
Vertical motion	ZT_L2	Upward	
Rotations:		**Island moving:**	
Around longitudinal axis	R_L2	Starboard down	
Around transverse axis	P_L2	Bow down	
Around vertical axis	Y_L2	Bow to portside	
MOTIONS OF DRIVING ISLAND L7 AT TARGET POSITION:			
Translations:		**Island moving:**	NDI optical measuring system
Longitudinal motion	XT_L7	Forward	
Transverse motion	YT_L7	To portside	
Vertical motion	ZT_L7	Upward	
Rotations:		**Island moving:**	
Around longitudinal axis	R_L7	Starboard down	
Around transverse axis	P_L7	Bow down	
Around vertical axis	Y_L7	Bow to portside	
MOTIONS OF DRIVING ISLAND L8 AT TARGET POSITION:			
Translations:		**Island moving:**	NDI optical measuring system
Longitudinal motion	XT_L8	Forward	
Transverse motion	YT_L8	To portside	
Vertical motion	ZT_L8	Upward	
Rotations:		**Island moving:**	
Around longitudinal axis	R_L8	Starboard down	
Around transverse axis	P_L8	Bow down	
Around vertical axis	Y_L8	Bow to portside	
MOTIONS OF DRIVING ISLAND L10 AT TARGET POSITION:			
Translations:		**Island moving:**	NDI optical measuring system
Longitudinal motion	XT_L10	Forward	
Transverse motion	YT_L10	To portside	
Vertical motion	ZT_L10	Upward	
Rotations:		**Island moving:**	
Around longitudinal axis	R_L10	Starboard down	
Around transverse axis	P_L10	Bow down	
Around vertical axis	Y_L10	Bow to portside	
MOTIONS OF DRIVING ISLAND L11 AT TARGET POSITION:			
Translations:		**Island moving:**	NDI optical measuring system
Longitudinal motion	XT_L11	Forward	
Transverse motion	YT_L11	To portside	
Vertical motion	ZT_L11	Upward	
Rotations:		**Island moving:**	
Around longitudinal axis	R_L11	Starboard down	
Around transverse axis	P_L11	Bow down	
Around vertical axis	Y_L11	Bow to portside	

TABLE 12 DESIGNATION, NOTATION, SIGN CONVENTION AND MEASURING DEVICE OF MEASURED QUANTITIES (V/IX)

Designation:	Notation:	Positive for:	Measured by:
MOTIONS OF DRIVING ISLAND L12 AT TARGET POSITION:			
Translations:		**Island moving:**	NDI optical measuring system
Longitudinal motion	XT_L12	Forward	
Transverse motion	YT_L12	To portside	
Vertical motion	ZT_L12	Upward	
Rotations:		**Island moving:**	
Around longitudinal axis	R_L12	Starboard down	
Around transverse axis	P_L12	Bow down	
Around vertical axis	Y_L12	Bow to portside	
MOTIONS OF DRIVING ISLAND L15 AT TARGET POSITION:			
Translations:		**Island moving:**	NDI optical measuring system
Longitudinal motion	XT_L15	Forward	
Transverse motion	YT_L15	To portside	
Vertical motion	ZT_L15	Upward	
Rotations:		**Island moving:**	
Around longitudinal axis	R_L15	Starboard down	
Around transverse axis	P_L15	Bow down	
Around vertical axis	Y_L15	Bow to portside	
MOTIONS OF DRIVING ISLAND L16 AT TARGET POSITION:			
Translations:		**Island moving:**	NDI optical measuring system
Longitudinal motion	XT_L16	Forward	
Transverse motion	YT_L16	To portside	
Vertical motion	ZT_L16	Upward	
Rotations:		**Island moving:**	
Around longitudinal axis	R_L16	Starboard down	
Around transverse axis	P_L16	Bow down	
Around vertical axis	Y_L16	Bow to portside	
MOTIONS OF DRIVING ISLAND S13 AT TARGET POSITION:			
Translations:		**Island moving:**	NDI optical measuring system
Longitudinal motion	XT_S13	Forward	
Transverse motion	YT_S13	To portside	
Vertical motion	ZT_S13	Upward	
Rotations:		**Island moving:**	
Around longitudinal axis	R_S13	Starboard down	
Around transverse axis	P_S13	Bow down	
Around vertical axis	Y_S13	Bow to portside	
MOTIONS OF DRIVING ISLAND S14 AT TARGET POSITION:			
Translations:		**Island moving:**	NDI optical measuring system
Longitudinal motion	XT_S14	Forward	
Transverse motion	YT_S14	To portside	
Vertical motion	ZT_S14	Upward	
Rotations:		**Island moving:**	
Around longitudinal axis	R_S14	Starboard down	
Around transverse axis	P_S14	Bow down	
Around vertical axis	Y_S14	Bow to portside	
MOTIONS OF DRIVING ISLAND S15 AT TARGET POSITION:			
Translations:		**Island moving:**	NDI optical measuring system
Longitudinal motion	XT_S15	Forward	
Transverse motion	YT_S15	To portside	
Vertical motion	ZT_S15	Upward	
Rotations:		**Island moving:**	
Around longitudinal axis	R_S15	Starboard down	
Around transverse axis	P_S15	Bow down	
Around vertical axis	Y_S15	Bow to portside	

TABLE 13 DESIGNATION, NOTATION, SIGN CONVENTION AND MEASURING DEVICE OF MEASURED QUANTITIES (VI/IX)

Designation:	Notation:	Positive for:	Measured by:
MOTIONS OF DRIVING ISLAND M1 AT TARGET POSITION:			
Translations:		**Island moving:**	NDI optical measuring system
Longitudinal motion	XT_M1	Forward	
Transverse motion	YT_M1	To portside	
Vertical motion	ZT_M1	Upward	
Rotations:		**Island moving:**	
Around longitudinal axis	R_M1	Starboard down	
Around transverse axis	P_M1	Bow down	
Around vertical axis	Y_M1	Bow to portside	
MOTIONS OF DRIVING ISLAND M2 AT TARGET POSITION:			
Translations:		**Island moving:**	NDI optical measuring system
Longitudinal motion	XT_M2	Forward	
Transverse motion	YT_M2	To portside	
Vertical motion	ZT_M2	Upward	
Rotations:		**Island moving:**	
Around longitudinal axis	R_M2	Starboard down	
Around transverse axis	P_M2	Bow down	
Around vertical axis	Y_M2	Bow to portside	
MOTIONS OF DRIVING ISLAND M12 AT TARGET POSITION:			
Translations:		**Island moving:**	NDI optical measuring system
Longitudinal motion	XT_M12	Forward	
Transverse motion	YT_M12	To portside	
Vertical motion	ZT_M12	Upward	
Rotations:		**Island moving:**	
Around longitudinal axis	R_M12	Starboard down	
Around transverse axis	P_M12	Bow down	
Around vertical axis	Y_M12	Bow to portside	
MOTIONS OF DRIVING ISLAND M13 AT TARGET POSITION:			
Translations:		**Island moving:**	NDI optical measuring system
Longitudinal motion	XT_M13	Forward	
Transverse motion	YT_M13	To portside	
Vertical motion	ZT_M13	Upward	
Rotations:		**Island moving:**	
Around longitudinal axis	R_M13	Starboard down	
Around transverse axis	P_M13	Bow down	
Around vertical axis	Y_M13	Bow to portside	
MOTIONS OF DRIVING ISLAND M14 AT TARGET POSITION:			
Translations:		**Island moving:**	NDI optical measuring system
Longitudinal motion	XT_M14	Forward	
Transverse motion	YT_M14	To portside	
Vertical motion	ZT_M14	Upward	
Rotations:		**Island moving:**	
Around longitudinal axis	R_M14	Starboard down	
Around transverse axis	P_M14	Bow down	
Around vertical axis	Y_M14	Bow to portside	
MOTIONS OF DRIVING ISLAND M15 AT TARGET POSITION:			
Translations:		**Island moving:**	NDI optical measuring system
Longitudinal motion	XT_M15	Forward	
Transverse motion	YT_M15	To portside	
Vertical motion	ZT_M15	Upward	
Rotations:		**Island moving:**	
Around longitudinal axis	R_M15	Starboard down	
Around transverse axis	P_M15	Bow down	
Around vertical axis	Y_M15	Bow to portside	

TABLE 14 DESIGNATION, NOTATION, SIGN CONVENTION AND MEASURING DEVICE OF MEASURED QUANTITIES (VII/IX)

Designation:	Notation:	Positive for:	Measured by:
MOTIONS OF DRIVING ISLAND M19 AT TARGET POSITION:			
Translations:		**Island moving:**	NDI optical measuring system
Longitudinal motion	XT_M19	Forward	
Transverse motion	YT_M19	To portside	
Vertical motion	ZT_M19	Upward	
Rotations:		**Island moving:**	
Around longitudinal axis	R_M19	Starboard down	
Around transverse axis	P_M19	Bow down	
Around vertical axis	Y_M19	Bow to portside	
MOTIONS OF DRIVING ISLAND M20 AT TARGET POSITION:			
Translations:		**Island moving:**	NDI optical measuring system
Longitudinal motion	XT_M20	Forward	
Transverse motion	YT_M20	To portside	
Vertical motion	ZT_M20	Upward	
Rotations:		**Island moving:**	
Around longitudinal axis	R_M20	Starboard down	
Around transverse axis	P_M20	Bow down	
Around vertical axis	Y_M20	Bow to portside	
MOTIONS OF DRIVING ISLAND M21 AT TARGET POSITION:			
Translations:		**Island moving:**	NDI optical measuring system
Longitudinal motion	XT_M21	Forward	
Transverse motion	YT_M21	To portside	
Vertical motion	ZT_M21	Upward	
Rotations:		**Island moving:**	
Around longitudinal axis	R_M21	Starboard down	
Around transverse axis	P_M21	Bow down	
Around vertical axis	Y_M21	Bow to portside	
MOTIONS OF DRIVING ISLAND M22 AT TARGET POSITION:			
Translations:		**Island moving:**	NDI optical measuring system
Longitudinal motion	XT_M22	Forward	
Transverse motion	YT_M22	To portside	
Vertical motion	ZT_M22	Upward	
Rotations:		**Island moving:**	
Around longitudinal axis	R_M22	Starboard down	
Around transverse axis	P_M22	Bow down	
Around vertical axis	Y_M22	Bow to portside	
MOTIONS OF DRIVING ISLAND M25 AT TARGET POSITION:			
Translations:		**Island moving:**	NDI optical measuring system
Longitudinal motion	XT_M25	Forward	
Transverse motion	YT_M25	To portside	
Vertical motion	ZT_M25	Upward	
Rotations:		**Island moving:**	
Around longitudinal axis	R_M25	Starboard down	
Around transverse axis	P_M25	Bow down	
Around vertical axis	Y_M25	Bow to portside	
MOTIONS OF DRIVING ISLAND M26 AT TARGET POSITION:			
Translations:		**Island moving:**	NDI optical measuring system
Longitudinal motion	XT_M26	Forward	
Transverse motion	YT_M26	To portside	
Vertical motion	ZT_M26	Upward	
Rotations:		**Island moving:**	
Around longitudinal axis	R_M26	Starboard down	
Around transverse axis	P_M26	Bow down	
Around vertical axis	Y_M26	Bow to portside	

TABLE 15 DESIGNATION, NOTATION, SIGN CONVENTION AND MEASURING DEVICE OF MEASURED QUANTITIES (VIII/IX)

Designation:	Notation:	Positive for:	Measured by:
MOTIONS OF DRIVING ISLAND M27 AT TARGET POSITION:			
Translations:		**Island moving:**	NDI optical measuring system
Longitudinal motion	XT_M27	Forward	
Transverse motion	YT_M27	To portside	
Vertical motion	ZT_M27	Upward	
Rotations:		**Island moving:**	
Around longitudinal axis	R_M27	Starboard down	
Around transverse axis	P_M27	Bow down	
Around vertical axis	Y_M27	Bow to portside	
MOTIONS OF DRIVING ISLAND M28 AT TARGET POSITION:			
Translations:		**Island moving:**	NDI optical measuring system
Longitudinal motion	XT_M28	Forward	
Transverse motion	YT_M28	To portside	
Vertical motion	ZT_M28	Upward	
Rotations:		**Island moving:**	
Around longitudinal axis	R_M28	Starboard down	
Around transverse axis	P_M28	Bow down	
Around vertical axis	Y_M28	Bow to portside	
MOTIONS OF DRIVING ISLAND M31 AT TARGET POSITION:			
Translations:		**Island moving:**	NDI optical measuring system
Longitudinal motion	XT_M31	Forward	
Transverse motion	YT_M31	To portside	
Vertical motion	ZT_M31	Upward	
Rotations:		**Island moving:**	
Around longitudinal axis	R_M31	Starboard down	
Around transverse axis	P_M31	Bow down	
Around vertical axis	Y_M31	Bow to portside	
MOTIONS OF DRIVING ISLAND M32 AT TARGET POSITION:			
Translations:		**Island moving:**	NDI optical measuring system
Longitudinal motion	XT_M32	Forward	
Transverse motion	YT_M32	To portside	
Vertical motion	ZT_M32	Upward	
Rotations:		**Island moving:**	
Around longitudinal axis	R_M32	Starboard down	
Around transverse axis	P_M32	Bow down	
Around vertical axis	Y_M32	Bow to portside	
MOTIONS OF DRIVING ISLAND M33 AT TARGET POSITION:			
Translations:		**Island moving:**	NDI optical measuring system
Longitudinal motion	XT_M33	Forward	
Transverse motion	YT_M33	To portside	
Vertical motion	ZT_M33	Upward	
Rotations:		**Island moving:**	
Around longitudinal axis	R_M33	Starboard down	
Around transverse axis	P_M33	Bow down	
Around vertical axis	Y_M33	Bow to portside	
MOTIONS OF THE VESSEL AT TARGET POSITION:			
Translations:		**Vessel moving:**	NDI optical measuring system
Longitudinal motion	X_TARGET	Forward	
Transverse motion	Y_TARGET	To portside	
Vertical motion	Z_TARGET	Upward	
Rotations:		**Vessel moving:**	
Around longitudinal axis	ROLL	Starboard down	
Around transverse axis	PITCH	Bow down	
Around vertical axis	YAW	Bow to portside	

TABLE 16 DESIGNATION, NOTATION, SIGN CONVENTION AND MEASURING DEVICE OF MEASURED QUANTITIES (IX/IX)

Designation:	Notation:	Positive for:	Measured by:
MOTIONS OF DRIVING ISLAND S4 AT TARGET POSITION:			
Translations:		**Island moving:**	NDI optical measuring system
Longitudinal motion	XT_S4	Forward	
Transverse motion	YT_S4	To portside	
Vertical motion	ZT_S4	Upward	
Rotations:		**Island moving:**	
Around longitudinal axis	R_S4	Starboard down	
Around transverse axis	P_S4	Bow down	
Around vertical axis	Y_S4	Bow to portside	
MOTIONS OF DRIVING ISLAND L4 AT TARGET POSITION:			
Translations:		**Island moving:**	NDI optical measuring system
Longitudinal motion	XT_L4	Forward	
Transverse motion	YT_L4	To portside	
Vertical motion	ZT_L4	Upward	
Rotations:		**Island moving:**	
Around longitudinal axis	R_L4	Starboard down	
Around transverse axis	P_L4	Bow down	
Around vertical axis	Y_L4	Bow to portside	

TABLE 17 DESIGNATION, NOTATION AND SIGN CONVENTION OF DERIVED QUANTITIES (I/VI)

Designation:	Notation:	Positive For:
MOTIONS OF DRIVING ISLAND L1 AT CENTRE OF GRAVITY:		
Translations:		**Island moving:**
Longitudinal motion	X_COG_L1	Forward
Transverse motion	Y_COG_L1	To portside
Vertical motion	Z_COG_L1	Upward
MOTIONS OF DRIVING ISLAND L2 AT CENTRE OF GRAVITY:		
Translations:		**Island moving:**
Longitudinal motion	X_COG_L2	Forward
Transverse motion	Y_COG_L2	To portside
Vertical motion	Z_COG_L2	Upward
MOTIONS OF DRIVING ISLAND L7 AT CENTRE OF GRAVITY:		
Translations:		**Island moving:**
Longitudinal motion	X_COG_L7	Forward
Transverse motion	Y_COG_L7	To portside
Vertical motion	Z_COG_L7	Upward
MOTIONS OF DRIVING ISLAND L8 AT CENTRE OF GRAVITY:		
Translations:		**Island moving:**
Longitudinal motion	X_COG_L8	Forward
Transverse motion	Y_COG_L8	To portside
Vertical motion	Z_COG_L8	Upward
MOTIONS OF DRIVING ISLAND L10 AT CENTRE OF GRAVITY:		
Translations:		**Island moving:**
Longitudinal motion	X_COG_L10	Forward
Transverse motion	Y_COG_L10	To portside
Vertical motion	Z_COG_L10	Upward
MOTIONS OF DRIVING ISLAND L11 AT CENTRE OF GRAVITY:		
Translations:		**Island moving:**
Longitudinal motion	X_COG_L11	Forward
Transverse motion	Y_COG_L11	To portside
Vertical motion	Z_COG_L11	Upward

TABLE 18 DESIGNATION, NOTATION AND SIGN CONVENTION OF DERIVED QUANTITIES (II/VI)

Designation:	Notation:	Positive For:
MOTIONS OF DRIVING ISLAND L12 AT CENTRE OF GRAVITY:		
Translations:		**Island moving:**
Longitudinal motion	X_COG_L12	Forward
Transverse motion	Y_COG_L12	To portside
Vertical motion	Z_COG_L12	Upward
MOTIONS OF DRIVING ISLAND L15 AT CENTRE OF GRAVITY:		
Translations:		**Island moving:**
Longitudinal motion	X_COG_L15	Forward
Transverse motion	Y_COG_L15	To portside
Vertical motion	Z_COG_L15	Upward
MOTIONS OF DRIVING ISLAND L16 AT CENTRE OF GRAVITY:		
Translations:		**Island moving:**
Longitudinal motion	X_COG_L16	Forward
Transverse motion	Y_COG_L16	To portside
Vertical motion	Z_COG_L16	Upward
MOTIONS OF DRIVING ISLAND S13 AT CENTRE OF GRAVITY:		
Translations:		**Island moving:**
Longitudinal motion	X_COG_S13	Forward
Transverse motion	Y_COG_S13	To portside
Vertical motion	Z_COG_S13	Upward
MOTIONS OF DRIVING ISLAND S14 AT CENTRE OF GRAVITY:		
Translations:		**Island moving:**
Longitudinal motion	X_COG_S14	Forward
Transverse motion	Y_COG_S14	To portside
Vertical motion	Z_COG_S14	Upward
MOTIONS OF DRIVING ISLAND S15 AT CENTRE OF GRAVITY:		
Translations:		**Island moving:**
Longitudinal motion	X_COG_S15	Forward
Transverse motion	Y_COG_S15	To portside
Vertical motion	Z_COG_S15	Upward
MOTIONS OF DRIVING ISLAND M1 AT CENTRE OF GRAVITY:		
Translations:		**Island moving:**
Longitudinal motion	X_COG_M1	Forward
Transverse motion	Y_COG_M1	To portside
Vertical motion	Z_COG_M1	Upward
MOTIONS OF DRIVING ISLAND M2 AT CENTRE OF GRAVITY:		
Translations:		**Island moving:**
Longitudinal motion	X_COG_M2	Forward
Transverse motion	Y_COG_M2	To portside
Vertical motion	Z_COG_M2	Upward

TABLE 19 DESIGNATION, NOTATION AND SIGN CONVENTION OF DERIVED QUANTITIES (III/VI)

Designation:	Notation:	Positive For:
MOTIONS OF DRIVING ISLAND M12 AT CENTRE OF GRAVITY:		
Translations:		**Island moving:**
Longitudinal motion	X_COG_M12	Forward
Transverse motion	Y_COG_M12	To portside
Vertical motion	Z_COG_M12	Upward
MOTIONS OF DRIVING ISLAND M13 AT CENTRE OF GRAVITY:		
Translations:		**Island moving:**
Longitudinal motion	X_COG_M13	Forward
Transverse motion	Y_COG_M13	To portside
Vertical motion	Z_COG_M13	Upward
MOTIONS OF DRIVING ISLAND M14 AT CENTRE OF GRAVITY:		
Translations:		**Island moving:**
Longitudinal motion	X_COG_M14	Forward
Transverse motion	Y_COG_M14	To portside
Vertical motion	Z_COG_M14	Upward
MOTIONS OF DRIVING ISLAND M15 AT CENTRE OF GRAVITY:		
Translations:		**Island moving:**
Longitudinal motion	X_COG_M15	Forward
Transverse motion	Y_COG_M15	To portside
Vertical motion	Z_COG_M15	Upward
MOTIONS OF DRIVING ISLAND M19 AT CENTRE OF GRAVITY:		
Translations:		**Island moving:**
Longitudinal motion	X_COG_M19	Forward
Transverse motion	Y_COG_M19	To portside
Vertical motion	Z_COG_M19	Upward
MOTIONS OF DRIVING ISLAND M20 AT CENTRE OF GRAVITY:		
Translations:		**Island moving:**
Longitudinal motion	X_COG_M20	Forward
Transverse motion	Y_COG_M20	To portside
Vertical motion	Z_COG_M20	Upward
MOTIONS OF DRIVING ISLAND M21 AT CENTRE OF GRAVITY:		
Translations:		**Island moving:**
Longitudinal motion	X_COG_M21	Forward
Transverse motion	Y_COG_M21	To portside
Vertical motion	Z_COG_M21	Upward
MOTIONS OF DRIVING ISLAND M22 AT CENTRE OF GRAVITY:		
Translations:		**Island moving:**
Longitudinal motion	X_COG_M22	Forward
Transverse motion	Y_COG_M22	To portside
Vertical motion	Z_COG_M22	Upward

TABLE 20 DESIGNATION, NOTATION AND SIGN CONVENTION OF DERIVED QUANTITIES (IV/VI)

Designation:	Notation:	Positive For:
MOTIONS OF DRIVING ISLAND M25 AT CENTRE OF GRAVITY:		
Translations:		**Island moving:**
Longitudinal motion	X_COG_M25	Forward
Transverse motion	Y_COG_M25	To portside
Vertical motion	Z_COG_M25	Upward
MOTIONS OF DRIVING ISLAND M26 AT CENTRE OF GRAVITY:		
Translations:		**Island moving:**
Longitudinal motion	X_COG_M26	Forward
Transverse motion	Y_COG_M26	To portside
Vertical motion	Z_COG_M26	Upward
MOTIONS OF DRIVING ISLAND M27 AT CENTRE OF GRAVITY:		
Translations:		**Island moving:**
Longitudinal motion	X_COG_M27	Forward
Transverse motion	Y_COG_M27	To portside
Vertical motion	Z_COG_M27	Upward
MOTIONS OF DRIVING ISLAND M28 AT CENTRE OF GRAVITY:		
Translations:		**Island moving:**
Longitudinal motion	X_COG_M28	Forward
Transverse motion	Y_COG_M28	To portside
Vertical motion	Z_COG_M28	Upward
MOTIONS OF DRIVING ISLAND M31 AT CENTRE OF GRAVITY:		
Translations:		**Island moving:**
Longitudinal motion	X_COG_M31	Forward
Transverse motion	Y_COG_M31	To portside
Vertical motion	Z_COG_M31	Upward
MOTIONS OF DRIVING ISLAND M32 AT CENTRE OF GRAVITY:		
Translations:		**Island moving:**
Longitudinal motion	X_COG_M32	Forward
Transverse motion	Y_COG_M32	To portside
Vertical motion	Z_COG_M32	Upward
MOTIONS OF DRIVING ISLAND M33 AT CENTRE OF GRAVITY:		
Translations:		**Island moving:**
Longitudinal motion	X_COG_M33	Forward
Transverse motion	Y_COG_M33	To portside
Vertical motion	Z_COG_M33	Upward
MOTIONS OF VESSEL AT CENTRE OF GRAVITY		
Translations:		**Vessel moving:**
Longitudinal motion	X_COG	Forward
Transverse motion	Y_COG	To portside
Vertical motion	Z_COG	Upward
MOTIONS OF DRIVING ISLAND S4 AT CENTRE OF GRAVITY:		
Translations:		**Island moving:**
Longitudinal motion	X_COG_S4	Forward
Transverse motion	Y_COG_S4	To portside
Vertical motion	Z_COG_S4	Upward
MOTIONS OF DRIVING ISLAND L4 AT CENTRE OF GRAVITY:		
Translations:		**Island moving:**
Longitudinal motion	X_COG_L4	Forward
Transverse motion	Y_COG_L4	To portside
Vertical motion	Z_COG_L4	Upward

TABLE 21 DESIGNATION, NOTATION AND SIGN CONVENTION OF DERIVED QUANTITIES (V/VI)

Designation:	Notation:	Positive For:
TOTAL FORCES AND MOMENTS OF L1-1 AROUND HEART FENDER:		
Longitudinal force	FX_L1-1	Forward
Transverse force	FY_L1-1	To portside
Vertical force	FZ_L1-1	Upward
Moment around longitudinal axis	MX_L1-1	Starboard down
Moment around transverse axis	MY_L1-1	Bow down
Moment around vertical axis	MZ_L1-1	Bow to portside
TOTAL FORCES AND MOMENTS OF L1-2 AROUND HEART FENDER:		
Longitudinal force	FX_L1-2	Forward
Transverse force	FY_L1-2	To portside
Vertical force	FZ_L1-2	Upward
Moment around longitudinal axis	MX_L1-2	Starboard down
Moment around transverse axis	MY_L1-2	Bow down
Moment around vertical axis	MZ_L1-2	Bow to portside
TOTAL FORCES AND MOMENTS OF L1-3 AROUND HEART FENDER:		
Longitudinal force	FX_L1-3	Forward
Transverse force	FY_L1-3	To portside
Vertical force	FZ_L1-3	Upward
Moment around longitudinal axis	MX_L1-3	Starboard down
Moment around transverse axis	MY_L1-3	Bow down
Moment around vertical axis	MZ_L1-3	Bow to portside
TOTAL FORCES AND MOMENTS OF L1-4 AROUND HEART FENDER:		
Longitudinal force	FX_L1-4	Forward
Transverse force	FY_L1-4	To portside
Vertical force	FZ_L1-4	Upward
Moment around longitudinal axis	MX_L1-4	Starboard down
Moment around transverse axis	MY_L1-4	Bow down
Moment around vertical axis	MZ_L1-4	Bow to portside
TOTAL FORCES AND MOMENTS OF L2-1 AROUND HEART FENDER:		
Longitudinal force	FX_L2-1	Forward
Transverse force	FY_L2-1	To portside
Vertical force	FZ_L2-1	Upward
Moment around longitudinal axis	MX_L2-1	Starboard down
Moment around transverse axis	MY_L2-1	Bow down
Moment around vertical axis	MZ_L2-1	Bow to portside
TOTAL FORCES AND MOMENTS OF L2-2 AROUND HEART FENDER:		
Longitudinal force	FX_L2-2	Forward
Transverse force	FY_L2-2	To portside
Vertical force	FZ_L2-2	Upward
Moment around longitudinal axis	MX_L2-2	Starboard down
Moment around transverse axis	MY_L2-2	Bow down
Moment around vertical axis	MZ_L2-2	Bow to portside

TABLE 22 DESIGNATION, NOTATION AND SIGN CONVENTION OF DERIVED QUANTITIES (VI/VI)

Designation:	Notation:	Positive For:
TOTAL FORCES AND MOMENTS OF M1-1 AROUND HEART FENDER:		
Longitudinal force	FX_L121	Forward
Transverse force	FY_L121	To portside
Vertical force	FZ_L121	Upward
Moment around longitudinal axis	MX_L121	Starboard down
Moment around transverse axis	MY_L121	Bow down
Moment around vertical axis	MZ_L121	Bow to portside
TOTAL FORCES AND MOMENTS OF M1-2 AROUND HEART FENDER:		
Longitudinal force	FX_L122	Forward
Transverse force	FY_L122	To portside
Vertical force	FZ_L122	Upward
Moment around longitudinal axis	MX_L122	Starboard down
Moment around transverse axis	MY_L122	Bow down
Moment around vertical axis	MZ_L122	Bow to portside
TOTAL FORCES AND MOMENTS OF M2-1 AROUND HEART FENDER:		
Longitudinal force	FX_L123	Forward
Transverse force	FY_L123	To portside
Vertical force	FZ_L123	Upward
Moment around longitudinal axis	MX_L123	Starboard down
Moment around transverse axis	MY_L123	Bow down
Moment around vertical axis	MZ_L123	Bow to portside
TOTAL FORCES AND MOMENTS OF M2-2 AROUND HEART FENDER:		
Longitudinal force	FX_L124	Forward
Transverse force	FY_L124	To portside
Vertical force	FZ_L124	Upward
Moment around longitudinal axis	MX_L124	Starboard down
Moment around transverse axis	MY_L124	Bow down
Moment around vertical axis	MZ_L124	Bow to portside

TABLE 23 OVERVIEW OF STATIC OFFSET TESTS

MARIN Test No. 30381_02OB_03_	Direction	Offset [m]	FX [kN]	Line 1 [kN]	Line 2 [kN]	Line 3 [kN]	Line 4 [kN]	Line 5 [kN]	Line 6 [kN]	Line 7 [kN]	Line 8 [kN]	Line 9 [kN]	Line 10 [kN]	Line 11 [kN]	Line 12 [kN]	Line 13 [kN]	Line 14 [kN]	Line 15 [kN]	Line 16 [kN]	Line 17 [kN]	Line 18 [kN]
002_001_02	WEST	0	22394	1855	1828	1776	1863	1871	1875	1872	1883	1895	1831	1840	1871	1874	1852	1828	1903	1892	1864
002_002_02		-10.8	60257	3963	3959	3851	3951	3977	3982	3973	4011	4034	3944	3968	3981	3956	3913	3893	4016	4039	3997
002_003_02		-21.6	291924	16576	16669	16796	16689	17212	16960	16873	16718	16665	17063	16852	16566	16549	16659	16998	16663	16688	16877
002_004_02		-10.8	60072	3930	3898	3818	3909	3910	3939	3933	3951	3997	3891	3919	3924	3902	3878	3847	3988	3981	3933
002_005_02		0	22425	1833	1808	1741	1851	1834	1856	1852	1875	1887	1819	1814	1855	1844	1843	1814	1893	1873	1829
002_006_02		9.6	11459	1240	1208	1150	1229	1229	1249	1241	1250	1271	1227	1206	1241	1234	1232	1204	1272	1251	1210
002_008_01		SWEEP 9.6 m to 0 m																			
002_009_01		SWEEP 0 to -21.6 m																			

MARIN Test No. ___0_	Direction	Offset [m]	FX [kN]	Line 19 [kN]	Line 20 [kN]	Line 21 [kN]	Line 22 [kN]	Line 23 [kN]	Line 24 [kN]	Line 25 [kN]	Line 26 [kN]	Line 27 [kN]	Line 28 [kN]
003_001_01	NORTH	0	-12658	1927	1903	1900	1908	1937	1861	1897	1889	1919	1893
003_002_01		-10.8	-5853	1239	1233	1217	1221	1242	1203	1218	1198	1220	1229
003_003_01		-21.6	-2990	956	944	930	933	950	910	924	909	933	933
003_004_01		-10.8	-5879	1247	1240	1219	1225	1244	1209	1224	1208	1229	1238
003_005_01		0	-12515	1918	1899	1892	1899	1939	1851	1889	1877	1913	1901
003_006_01		9.6	-29628	3652	3641	3619	3625	3590	3552	3580	3598	3650	3606
003_007_01		SWEEP 9.6 m to -21.6 m											

MARIN Test No. ___0_	Direction	Offset [m]	FX [kN]	Line 29 [kN]	Line 30 [kN]	Line 31 [kN]	Line 32 [kN]	Line 33 [kN]	Line 34 [kN]	Line 35 [kN]	Line 36 [kN]
004_001_01	EAST	0	-24192	3700	3596	3632	3615	3611	3641	3588	3665
004_002_01		-10.8	-9385	1835	1788	1800	1796	1785	1792	1750	1795
004_003_01		-21.6	-4477	1210	1172	1187	1187	1171	1182	1160	1188
004_004_01		-10.8	-9387	1841	1787	1807	1801	1782	1796	1769	1808
004_005_01		0	-24109	3703	3595	3644	3620	3619	3636	3586	3670
004_006_01		9.6	-91372	12265	11990	12060	12065	11957	11942	11670	11973
004_007_01		SWEEP 9.6 m to -21.6 m									

MARIN Test No. ___0_	Direction	Offset [m]	FX [kN]	Line 37 [kN]	Line 38 [kN]	Line 39 [kN]	Line 40 [kN]	Line 41 [kN]	Line 42 [kN]	Line 43 [kN]	Line 44 [kN]	Line 45 [kN]	Line 46 [kN]
005_001_01	SOUTH	0	12272	1869	1878	1922	1860	1869	1868	1881	1883	1815	1927
005_002_01		-10.8	32915	3932	3962	4004	3931	3898	3940	3941	3939	3939	3972
005_003_01		-21.6	165829	17431	17323	17400	17425	17536	17404	17175	16668	16914	16686
005_004_01		-10.8	32625	3871	3905	3933	3859	3819	3869	3855	3888	3883	3905
005_005_01		0	12049	1839	1853	1888	1821	1825	1822	1839	1858	1776	1881
005_006_01		9.6	5945	1246	1253	1295	1228	1231	1222	1237	1261	1164	1270
005_007_02		SWEEP 9.6 m to -21.6 m											

TABLE 24 OVERVIEW OF TESTS IN IRREGULAR WAVES

MARIN Test No. 30381_02OB_05_	Test	Time [h]	Wave Characteristics				Current	
			Hs [m]	Tp [s]	Dir. [deg]	γ [-]	Vc [m/s]	Dir. [deg]
without current								
003_001_01	Operational 180	½ + 3	2.0	5.50	180	3.30	-	-
004_001_01	Operational 210			6.50	210			
005_001_01	Operational 225			7.50	225			
006_001_01	1yr 180		3.0	6.50	180			
007_001_01	1yr 210			7.50	210			
008_001_01	1yr 225			8.00	225			
009_001_01	10yr 180		5.0	8.0	180			
010_001_01	10yr 210				210			
011_001_01	100yr 180		5.9	10.5	180			

TABLE 25 OVERVIEW OF TESTS IN IRREGULAR WAVES

MARIN Test No. 30381_02OB_06_	Test	Time [h]	Wave Characteristics				Current	
			Hs [m]	Tp [s]	Dir. [deg]	γ [-]	Vc [m/s]	Dir. [deg]
with current								
012_001_01	Operational 180	½ + 3	2.0	5.50	180	3.30	1.00	180
013_001_01	Operational 210			6.50	210			
014_001_01	Operational 225			7.50	225			
015_001_01	1yr 180		3.0	6.50	180			
016_001_01	1yr 210			7.50	210			
017_001_01	1yr 225			8.00	225			
018_001_01	10yr 180		5.0	8.0	180			
019_001_01	10yr 210				210			
020_001_02	100yr 180		5.9	10.5	180			
001_002_01	Current only	1	-	-	-	-		
001_002_02								

TABLE 26 OVERVIEW OF TESTS IN IRREGULAR WAVES

MARIN Test No. 30381_02OB_07_	Test	Time [h]	Wave Characteristics				Current	
			Hs [m]	Tp [s]	Dir. [deg]	γ [-]	Vc [m/s]	Dir. [deg]
003_001_01	Operational 180	½ + 3	2.0	5.50	180	3.30	-	-
004_001_01	Operational 210			6.50	210			
005_001_01	Operational 225			7.50	225			
006_001_01	1yr 180		3.0	6.50	180			
007_001_01	1yr 210			7.50	210			
008_001_01	1yr 225			8.00	225			

FIGURES

FIGURE 1 LABELLING OF MODULES AND MOORING LINES

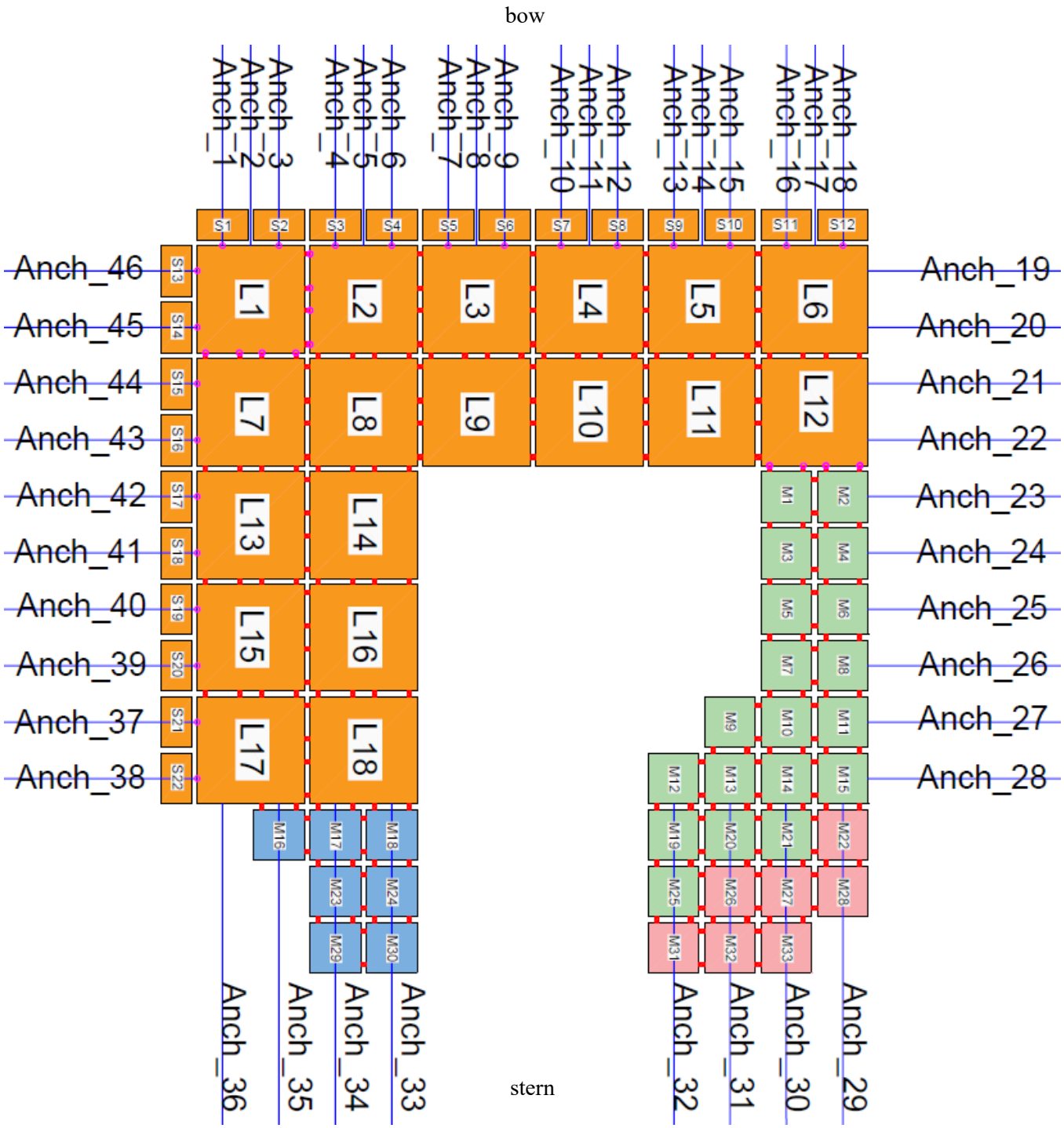

APPENDICES

APPENDIX D01

Methods to Determine Damping Coefficients from the Results of Motion Decay Tests

Revision	Date	Description of revision	Author
0	September 10, 2009	First version of the appendix	JH
1	February 24, 2010	Minor corrections in wording and equations	JvdB
2	January 28, 2011	Units and eq. damping formulation added	JJS
3	September 13, 2017	Typo's corrected	FJ
4	November 12, 2018	Adjusted to SHARK	AN

DECAY TESTS, DETERMINING DAMPING AND PERIODICITY

Decay/free extinction tests are performed to determine the damping coefficients, damped period and natural period of a floater or system. Decaying signals are characterised by a decaying oscillation around a mean value, with an approximately constant period. An example of a decaying signal is shown below:

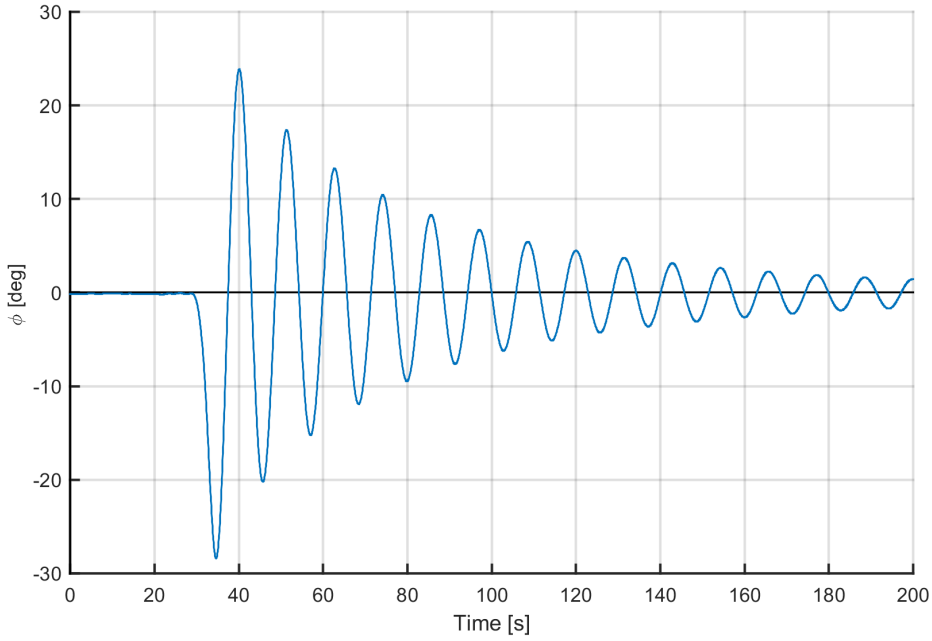

Time series of decaying roll signal

It is assumed that the decaying system can be accurately described by the following equation:

$$a\ddot{x} + b(\dot{x}) + cx = 0 \qquad (1)$$

Where:

- x is a motion signal (e.g. roll, pitch or heave)
- $\dot{x}$ is the first derivative of the motion signal (e.g. roll velocity)
- $\ddot{x}$ is the second derivative (e.g. roll acceleration)
- *a* is the mass or inertia of the floater (including added mass or added inertia)
- *c* is the restoring term of the floater
- *b()* is the damping function

The damping function can have various terms. The following terms are implemented for analysis at MARIN:

$$b(\dot{x}) = B_1\dot{x} + B_2\dot{x}|\dot{x}| + B_3\dot{x}^3 \qquad (2)$$

Where:

- B_1 is the linear damping coefficient
- B_2 is the quadratic damping coefficient
- B_3 is the cubic damping coefficient

Solving only for B_1 is called the "first order solution", solving for B_1 and B_2 is called the "second order solution" and solving for B_1, B_2 and B_3 is called the "third order solution". In very rare cases B_1 and B_3 can be determined while leaving B_2 zero. This is called the "13 order solution". Usually the second order solution is used. Only when a damping test clearly shows cubic behaviour is the third term determined as well.

Analysis of a motion signal alone does not provide absolute damping coefficients; it only provides relative damping coefficients in the form B/c. An absolute value of c has to be provided before an absolute value of B can be found. As an example, c can be defined as $g\square GM$ for a roll decay.

The relative damping can be analysed by three methods. First, Equation 1 can be solved by inserting the measured motion, velocity and acceleration and solving in a least squared sense. This is called the "least squares fit". Secondly, classic "PQ analysis" can be performed. PQ analysis sets out all individual crests and troughs as a function of amplitude and fits a polynomial through. The polynomial coefficients are denoted by P and Q (and R in the cubic damping case). Lastly, the motion signal itself can be fit in an optimal sense by varying the relative damping and natural period of the system until an optimum is found. This is called "motion optimised".

All three methods determine the same relative damping values, but with different approaches to what is optimal. The classic PQ analysis works very well for lightly damped systems, but has difficulties to provide accurate values for highly damped systems (e.g. ships sailing at speed). The least squares fit and motion optimised methods are closely related. The motion optimised method actually removes the need for fitting velocity and acceleration in the system of equations, which sometimes caused irregularities in the fitting.

The decay analysis results can be verified using a PQ-diagram, a recalculation of the time series and via a plot of the damped period per oscillation.

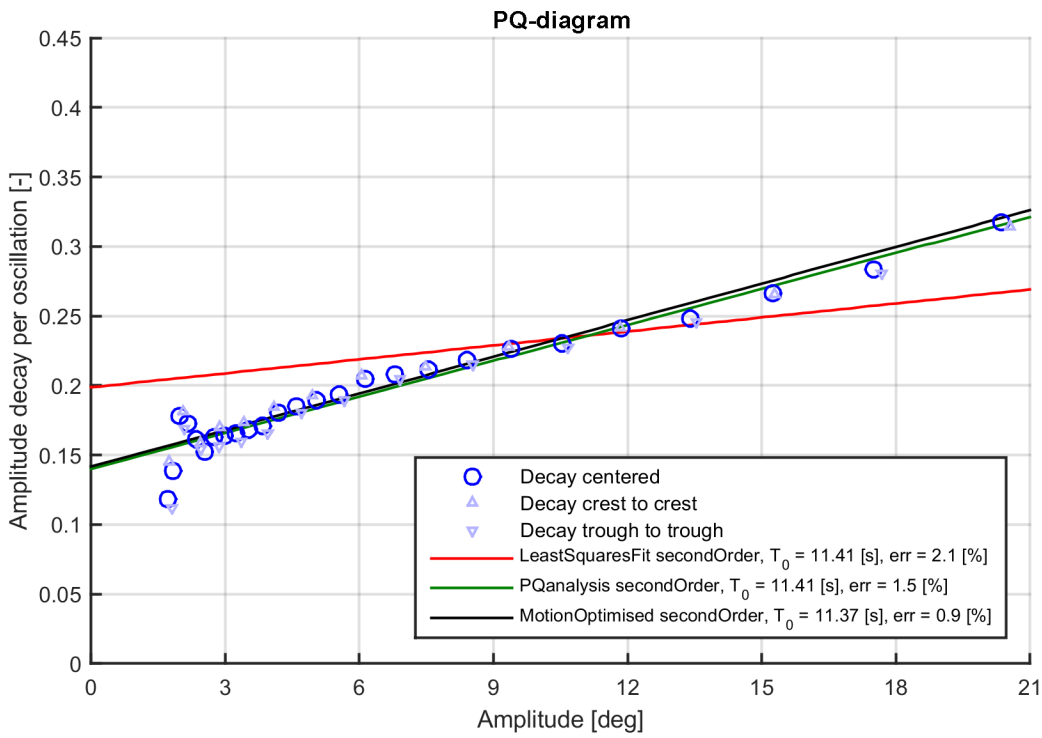

Example of a PQ-diagram showing all three methods

The PQ-diagram shows the decay of the crests and troughs in three ways. "Decay centred" shows the amplitude decay calculated as the difference between two consecutive crest-trough differences or trough-

crest differences. This method is not sensitive to offsets in the signal. These values are also used in the PQ analysis method. The "crest to crest" and "trough to trough" decays are provided to indicate offsets and other irregularities in the signal. Ideally all three should coincide. In this case the second order results of all three fitting methods are indicated. Normally the best fitting method is used and the others are not shown.

The damping coefficients B_1, B_2, B_3 and P, Q, R values translate into one another as follows; see also "Slingergedrag van Schepen" door Ir J.J.W. van der Vegt, "KIVI-zeegangsdag", March 1 1984:

$$\frac{B_1}{c} = \frac{PT_0}{2\pi^2}$$
$$\frac{B_2}{c} = \frac{3QT_0^2}{32\pi^2} \qquad (3)$$
$$\frac{B_3}{c} = \frac{RT_0^3}{6\pi^4}$$

Where:

- P, Q and R are the zeroth, first and second order polynomial components of the fit of crest and trough decay
- T_0 is the natural or undamped period of the system

Ideally the natural period can be expressed as:

$$T_0 = 2\pi\sqrt{\frac{a}{c}} \qquad (4)$$

The damped period T_d is the observed period and can change slightly with oscillation amplitude. In the case of an ideal linear damped system the damped and natural periods are related via:

$$T_0 = T_d\sqrt{1-\zeta^2}$$
$$\zeta = \frac{B_1}{2\sqrt{ac}} \qquad (5)$$

Where:

- ζ is the damping ratio

T_d and hence T_0 is (initially) determined from the mean crossings of the signal; however, it is further optimised when the motion optimised method is used.

The error mentioned in the legend of the PQ-diagram is actually the error function used in the motion optimised method, which is the L2-norm of the difference between the measured motion and the recalculated motion after fitting. An example of the recalculation is shown in the next figure:

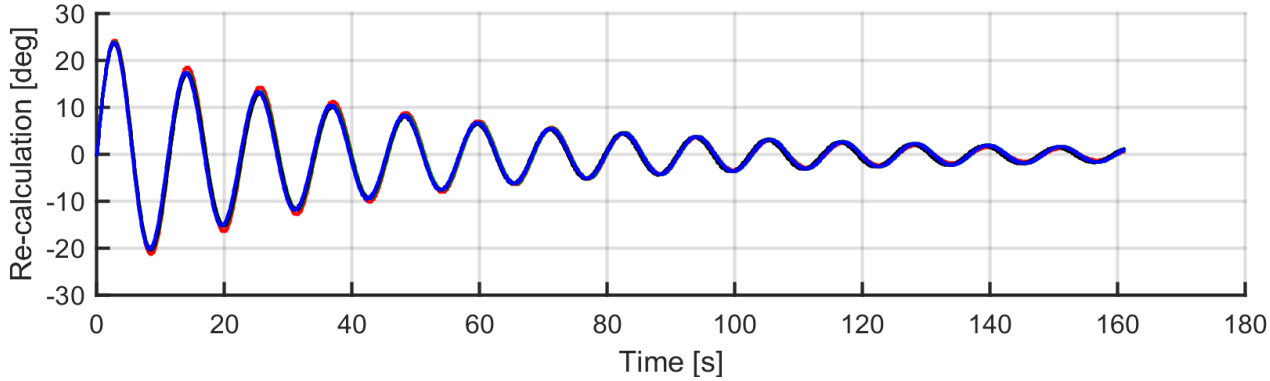

Example of a recalculation showing all three methods; the original signal is shown in blue

The recalculation diagram can be used to check whether the periods found and damping actually match with the measured signal. In this case the red line of the least square fit method shows too little damping at the beginning of the time series at large oscillation amplitudes and somewhat too much damping at the end of the time series. This was also indicated in the PQ-diagram. The other methods fit relatively accurate to the measured data.

The behaviour of the damped period is shown as a function of the number of oscillations as shown below:

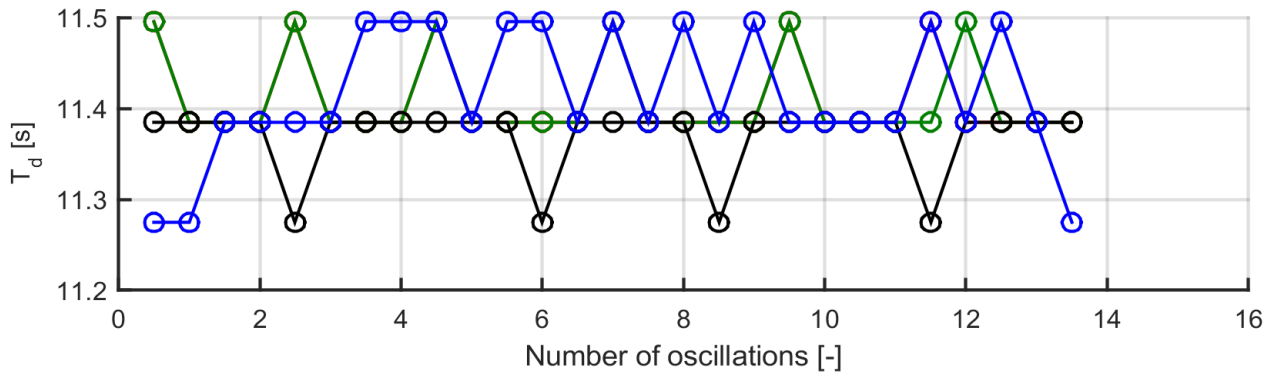

Example of a period overview; the original signal is shown in blue

This plot can be used to check for errors in the mean crossings (e.g. when a poorly conditioned signal has erratic mean crossings the average period estimate will be too small). In this case both the original signal and the three methods are in agreement and show a very constant damped period.

APPENDIX D02

Mathematical Description of Irregular Phenomena

Revision	Date	Description of revision	Author
0	May 19, 2009	First version of the appendix	JLC

Mathematical Description of Irregular Phenomena

General

A quantity x, varying irregularly in time or space is called a stochastic variable. The stochastic variables that are most interesting in the field of seakeeping are varying in time and can each be described by a distribution function of the probability that x fulfils a certain condition. Examples of such distribution functions are (see Figure A):

1. The probability distribution for the period of time that the value x lies between a and b.
2. The probability distribution of amplitudes of x lying between a and b.

Figure A

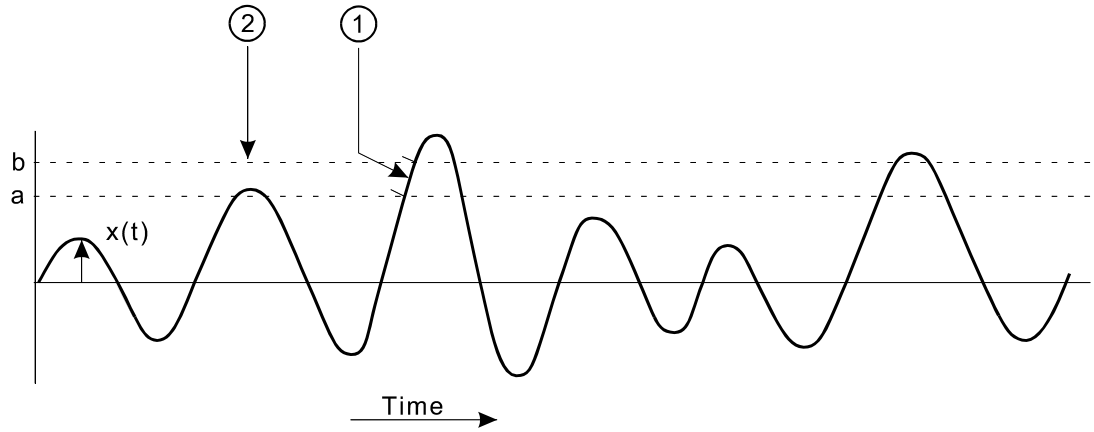

These various descriptions are discussed under the following subheadings. Before doing so, it is necessary to mention a few characteristics to classify random processes.

A process, described by a stochastic variable x, is completely defined if all statistical properties are known, or to be precise, when the expectation values E[x], E[x^2], E[x^3], ... are all known. In general this is not the case.

Processes can be classified by certain properties of their statistics. If for a process all statistical properties are invariant with respect to time shifts, the process is called ***stationary***. This means, for example, that:

$$E[x(t)] = E[x(t+\tau)] \qquad -\infty < \tau < \infty \tag{1}$$

E[x] is the ***mean value*** of x, also denoted by $\bar{x}$.

The statistical properties of a random process can be measured in several ways, depending on the character of the process. For instance, assume a sea with a large number of wave height measuring buoys of the same type, measuring simultaneously. The mean value of the wave elevations is established as the average of the registration of all buoys at time $t = t_m$. Now, the actual waves at sea are a weakly stationary process; in case of long periods of time the expectation values are not time invariant, but for practical purposes the wave elevation (and as a result: ship motions) can be considered as stationary processes.

A stationary process is called ergodic when it is allowed to replace the averaging over space by an averaging over time and to use the registration of one single buoy for the characterization of the sea state, as described above, or to use one ship model to measure its motions.

Probability distribution of x(t)

The wave elevations are a continuous function of time (see Figure A) and the probability that $a \le x \le b$ is given by the probability density function $p_x(y)$ in such a way that:

$$P[a \le x \le b] = \int_a^b p_x(y)\,dy$$

where:

$$\int_{-\infty}^{\infty} p_x(y)\,dy = 1 \qquad (2)$$

If the process has a normal (Gaussian) distribution the probability density function is:

$$p(x) = \frac{1}{\sigma_x \sqrt{2\pi}} . \exp\left[-\frac{(x - \bar{x})^2}{2\sigma_x^2} \right] \qquad (3)$$

in which:

$\bar{x}$ = E[x], the mean value, and
σ_x = the standard deviation of the process

The standard deviation is defined as the root of the variance and:

$$\sigma_x^2 = VAR. = E[x - E[x]]^2 = E[x^2] - (E[x])^2 \qquad (4)$$

Now it is possible to calculate for a normal distributed stochastical variable x the probability that, for instance, $(\bar{x} + \frac{n}{2}\sigma_x) \le x \le (\bar{x} + \frac{n+1}{2}\sigma_x)$ for several values of n. The result is shown in the histogram in Figure B on the next page. Note that the mean value not necessarily coincides with the point of reference in the measuring system, so in the above definition of a Gaussian distribution x is given relative to $\bar{x}$.

Figure B: Normalised Gaussian distribution

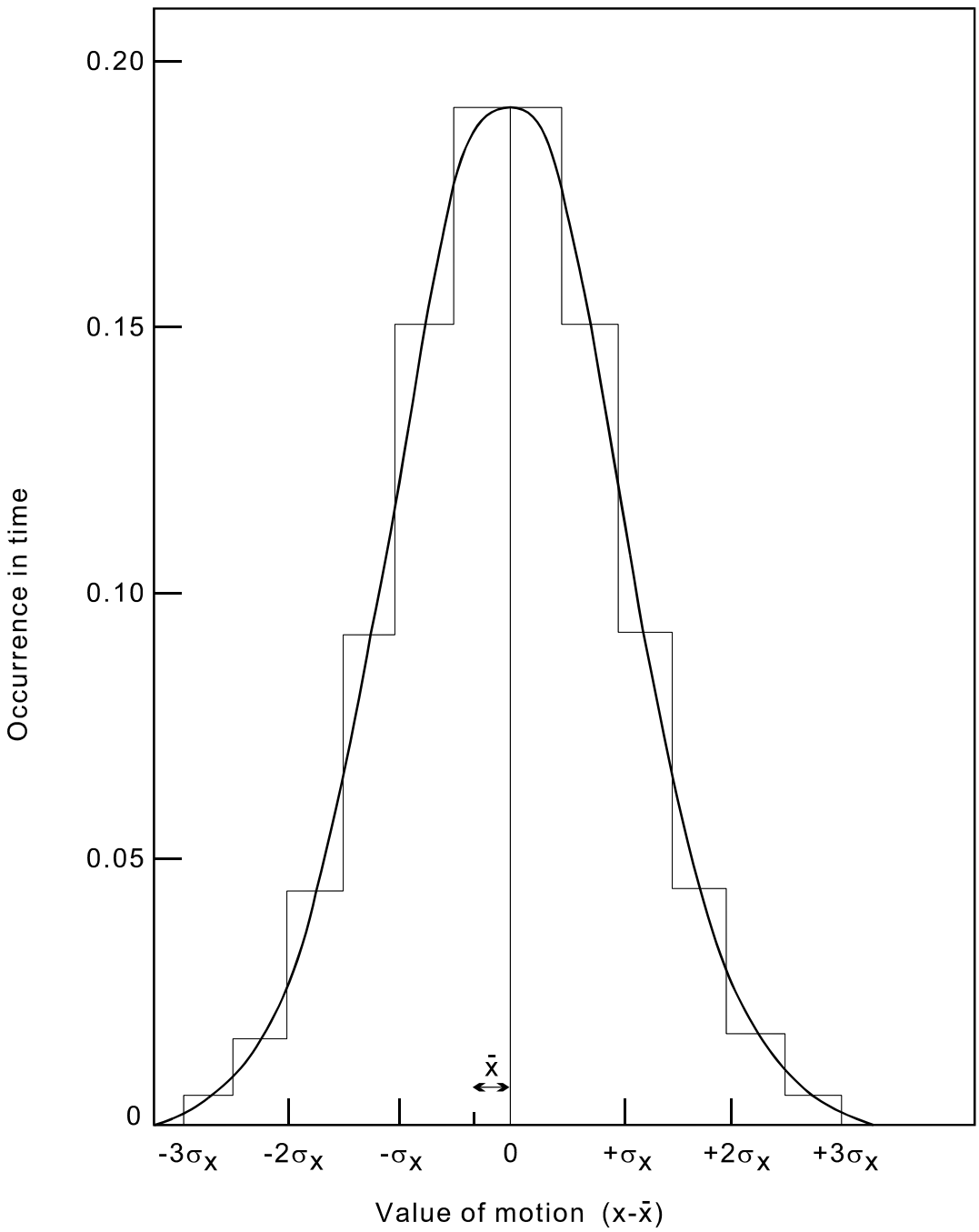

NOTE: width of the columns in the histogram = ½σ_x
σ_x = standard deviation of the variable x

The probability that the value for $(x - \bar{x})$ exceeds a certain level x_m can be expressed as:

$$P[x_m \leq (x - \bar{x}) < \infty] = \int_{x_m + \bar{x}}^{\infty} p_x(y)\, dy \tag{5}$$

Using (3), (4) and (5) the following table gives results for several values of x_m.

x_m	Probability percentage $P[x_m \leq x < \infty]$	Probability percentage $P[-\infty < x \leq x_m]$
$\bar{x} - 3\sigma_x$	99.87	0.13
$\bar{x} - 2\sigma_x$	97.72	2.28
$\bar{x} - 1\sigma_x$	84.10	15.90
$\bar{x} + 1\sigma_x$	15.90	84.10
$\bar{x} + 2\sigma_x$	2.28	97.72
$\bar{x} + 3\sigma_x$	0.13	99.87

Probability distribution of amplitudes of x(t)

Additionally, the stochastic variable x can be described by the distribution of the amplitudes (= peak values) of x. When x has a normal distribution, the amplitudes follow a Rayleigh distribution. As regards these amplitudes, which are the most interesting quantities in the measurement of ship motions, several stochastic quantities can be defined. When:

x_a ≡ the amplitude of $[x - \bar{x}]$, then:

$x_{a1/3}$ ≡ the mean of the highest one-third of the amplitudes of x_a, or as it is often called: the significant single amplitude of x;

$2x_{a1/3}$ ≡ mean of the highest one-third of the maximum to minimum values of x_a, often called: the significant double amplitude of x

Then the most probable maximum value $2x_{a\,max.}$ (double amplitude) of the variable x depends on the number of oscillations N_o, as calculated by Longuet-Higgins[1)].

$$2x_{a\,max.} = 2\sigma_x \sqrt{2\theta} \tag{6}$$

with:

$$\theta = \ln N_o - \ln\left[1 - \frac{1}{2\theta}(1 - e^{-\theta})\right] \tag{7}$$

1) Longuet-Higgins, M.S.; "On the Statistical Distribution of the Heights of Sea Waves", Journal of Marine Research 1952, Number 3.

For large values of N_o it can be shown that:

$$2x_{a\,max.} = 2\sigma_x \sqrt{2 \ln N_o} \tag{8}$$

In actual measurements, the registration of x over a period of time is used. This period of time has to be long enough to give a reliable estimate of the statistical properties of the variable x as well as for the above introduced stochastical variables $x_{a1/3}$ and $2x_{a1/3}$. (It is generally accepted to be sufficient when this period corresponds to half an hour real time or includes at least 180 oscillations). Then, the mean value is given by:

$$E[x] = \bar{x} = \frac{1}{T} \int_{t_1}^{t_2} x(t)\,dt \qquad \text{with } T = t_2 - t_1$$

and the standard deviation is:

$$\sigma_x = \sqrt{\frac{1}{T} \int_{t_1}^{t_2} [x(t) - \bar{x}]^2\,dt}$$

The observed processes are stationary - or at least weakly stationary - and ergodic. So the above described simplifications for the establishment of $\bar{x}$ and σ_x are allowed. When the duration of the measurement is sufficiently long, the difference between the standard deviation of the sample and the standard deviation of the actual density function can be neglected. The probability functions actually found from sampling an experiment generally conform very well with the theoretical distributions for x-values in the vicinity of $\bar{x}$. Due to the limited sample size the agreement at x-values far from $\bar{x}$ is hard to prove.

Spectral density of x

When the stochastic quantity x, varying irregularly in time t ($0 \le t < T$ with $T \to \infty$), is plotted as a function of time and its variations between t and t + Δt are bounded for $\Delta t \to 0$, then x(t) can be represented by an infinite number of harmonic components with arbitrary phase angles:

$$x(t) = x_0 + \sum_{n=1}^{\infty} x_n \cos(\omega_n t + \varepsilon_n) \qquad \text{(Fourier series)} \tag{9}$$

in which:

x_n	=	the amplitude of harmonic component n
ε_n	=	phase angle of the n-th component
ω_n	=	$n\omega_1$ = angular frequency of the n-th harmonic component
ω_1	=	$2\pi/T$ (T = measuring time)

and so: $x_0 = \bar{x}$ the mean value of x.

Now, suppose there is a stationary, ergodic process, described by the stochastic variable $x_T(t)$ of which the observation takes place over a time interval ($-T < t < T$, $T \to \infty$), as shown in Figure C.

Figure C

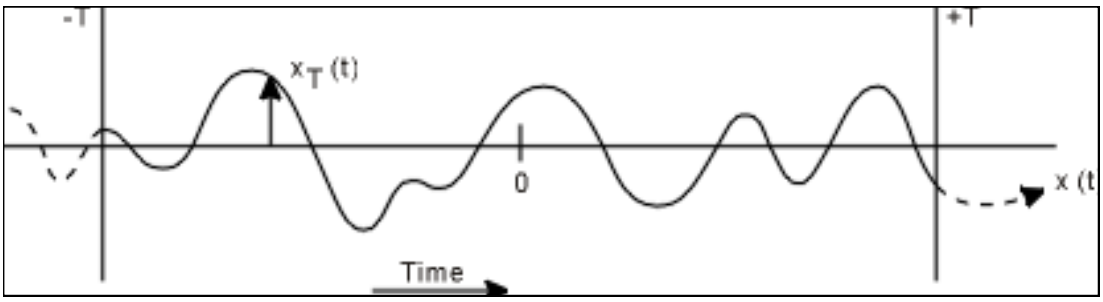

Then the Fourier series can be replaced by the Fourier transformation and the following relations result:

$$X_T(\omega) = \int_{-\infty}^{\infty} x_T(t)\, e^{-i\omega t}\, dt = \int_{-T}^{T} x(t)\, e^{-i\omega t}\, dt \tag{10}$$

$$x_T(t) = \frac{1}{2\pi} \int_{-\infty}^{\infty} X_T(\omega)\, e^{+i\omega t}\, d\omega \quad \text{(inverse Fourier transformation)}$$

The mean value and mean square value (= standard deviation when $\bar{x} = 0$) are defined as follows:

$$\bar{x} = \lim_{T\to\infty} \frac{1}{2T} \int_{-\infty}^{\infty} x_T(t)\, dt = \lim_{T\to\infty} \frac{1}{2T} \int_{-T}^{T} x(t)\, dt \tag{11}$$

$$\bar{M}_x = \lim_{T\to\infty} \frac{1}{2T} \int_{-\infty}^{\infty} \{x_T(t)\}^2\, dt = \lim_{T\to\infty} \frac{1}{2T} \int_{-T}^{T} \{x(t)\}^2\, dt \tag{12}$$

The spectral density function $S_{xx}(\omega)$ of the random process $x_T(t)$ can be proven to be[2)]:

$$S_{xx}(\omega) = \lim_{T\to\infty} \frac{1}{2\pi T} |X_T(\omega)|^2 \tag{13}$$

Using Parceval's theorem on Fourier transformations[3)], the mean square can be expressed in terms of frequency:

$$\overline{M}_x = \lim_{T\to\infty} \frac{1}{2T} \left\{ \frac{1}{2\pi} \int_{-\infty}^{\infty} |X_T(\omega)|^2 \, d\omega \right\} = \frac{1}{2} \int_{-\infty}^{\infty} S_{xx}(\omega) \, d\omega \tag{14}$$

The spectral density function can be related to the energy W which will be clarified in the following discussion. The Fourier transformation $X_T(\omega)$ is the continuous representation of the amplitudes x_n in the Fourier series of $x_T(t)$. Now, the potential energy E_n of the component with frequency ω_n is proportional with $(x_n)^2$ and analogously the potential energy in the frequency range of $\omega_i \le \omega \le \omega_j$ is:

$$W(\omega_i \le \omega \le \omega_j) \_ \int_{\omega_i}^{\omega_j} |X_T(\omega)|^2 \, d\omega$$

and the average potential energy over a period of time is, using (13):

$$W \sim \lim_{T\to\infty} \frac{1}{T} [W(\omega_i \le \omega \le \omega_j)] = \int_{\omega_i}^{\omega_j} S_{xx}(\omega) \, d\omega \tag{15}$$

So, the average potential energy of $x_T(t)$, associated with the frequency band $\omega_i \le \omega \le \omega_j$ is given by the integral of $S_{xx}(\omega)$ over the frequency interval and hence $S_{xx}(\omega)$ may be called the ***energy spectral density function.***

---

2) Therefore use is made of the auto-covariance function $R_{xx}(\tau)$, defined as:

$$R_{xx}(\tau) = E[\{x(t) - E[x(t)]\} . \{x(s) - E[x(s)]\}]$$

with $\tau = s - t$. In the representation of this section, with $\overline{x} = 0$, is:

$$R_{xx}(\tau) = \lim_{T\to\infty} \frac{1}{2T} \int_{-\infty}^{\infty} x_T(t) \, x_T(t+\tau) \, dt$$

Now, $S_{xx}(\omega)$ is defined as the Fourier transformation of the auto-covariance function: $S_{xx}(\omega) = \frac{1}{\pi} \int_{-\infty}^{\infty} R_{xx}(\tau) \, e^{-i\omega\tau} \, dt$

3) This theorem states that:

$$\int_{-\infty}^{\infty} \{x(t)\}^2 \, dt = \frac{1}{2\pi} \int_{-\infty}^{\infty} |X(\omega)|^2 \, d\omega$$

The concept of response

Mechanical and physical systems may be interpreted as a transducer transmitting energy from the input x(t) towards the output or response y(t). Suppose the output is uniquely determined in terms of the input: y(t) = L[x(t)], then the system is completely defined if the nature of the operator L is known. The spectral density representation of a stochastic variable allows an output density function $S_{yy}(\omega)$ to the input density $S_{xx}(\omega)$ by means of a frequency response function, provided that the observed system is linear[4]. Consider the situation where the unit impulse, described by the Dirac delta function[5] $\delta(t - t_0)$, is applied at time $t = t_0$ to a linear system and let $h(t - t_0)$ be the response of the system: $L[\delta(t - t_0)] = h(t - t_0)$. Because such an input-output system is causal, $h(t - t_0)$ does not exist for $t_0 > t$. Now, an arbitrary input x(t) can be expressed as a sum of impulses, that is:

$$x(t) = \int_{-\infty}^{t} x(t_0)\,\delta(t - t_0)\,dt_0 \tag{16}$$

---

4) A system is linear if the response characteristics are additive and homogeneous:

$L[x_1(t) + x_2(t)] = L[x_1(t)] + L[x_2(t)] = y_1(t) + y_2(t)$

$L[ax(t)] = aL[x(t)] = ay(t)$ (a = constant).

5) The Dirac function or "unit impulse function" is an infinitely sharp peak function with the following character:

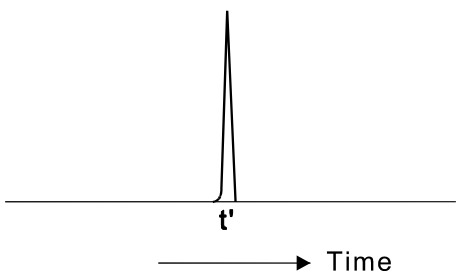

$\delta(t - t') = 0$ for $t \neq t'$

and:

$$\int_{t'-\varepsilon}^{t'+\varepsilon} \delta(t - t')\,dt = 1 \quad \text{for } \varepsilon \to +0$$

and:

$$\int_{-\infty}^{\infty} x(t)\,\delta(t - t')\,dt = x(t').$$

in which case, assuming that L is time-invariant:

$$y(t) = L[x(t)] = \int_{-\infty}^{t} x(t_0)\, L[\delta(t-t_0)]\, dt_0 = \int_{-\infty}^{t} x(t_0)\, h(t-t_0)\, dt_0 =$$
$$= \int_{0}^{\infty} x(t-\tau)\, h(\tau)\, d\tau$$

where: $t - t_0 = \tau$ was substituted.

For the truncated variables $x_T(t)$ and $y_T(t)$ as used before, with their Fourier transformations $X_T(\omega)$ and $Y_T(\omega)$ it is thus found that:

$$y_T(t) = \int_{0}^{\infty} x_T(t-\tau)\, h(\tau)\, d\tau \tag{17}$$

and:

$$\begin{aligned} Y_T(\omega) &= \int_{-\infty}^{\infty} e^{-i\omega t} \left[\int_{0}^{\infty} x_T(t-\tau)\, h(\tau)\, d\tau \right] dt \\ &= \int_{0}^{\infty} h(\tau) \left[\int_{-\infty}^{\infty} e^{-i\omega t}\, x_T(t-\tau)\, dt \right] d\tau \\ &= \int_{0}^{\infty} h(\tau) \left[\int_{-\infty}^{\infty} x_T(u)\, e^{-i\omega u} du \right] e^{-i\omega\tau}\, d\tau \\ &= X_T(\omega) \int_{0}^{\infty} h(\tau)\, e^{-i\omega\tau}\, d\tau \\ &\equiv X_T(\omega)\, H(\omega) \end{aligned} \tag{18}$$

in which $u = t - \tau$.

$H(\omega)$ is the Fourier transformation of $h(t)$ and is called the frequency response function. Using the definition for the spectral density function (13), it follows that for real processes $x_T(t)$ and $y_T(t)$:

$$S_{yy}(\omega) = \lim_{T\to\infty} \frac{1}{2\pi T} |Y_T(\omega)|^2 = \lim_{T\to\infty} \frac{1}{2\pi T} |X_T(\omega)|^2 |H(\omega)|^2$$

and thus:

$$S_{yy}(\omega) = S_{xx}(\omega) |H(\omega)|^2 \tag{19}$$

So, the relation is derived that the output spectral density function is equal to the product of the input spectral density function and the square of the frequency response function.

In a graphic representation:

Figure D

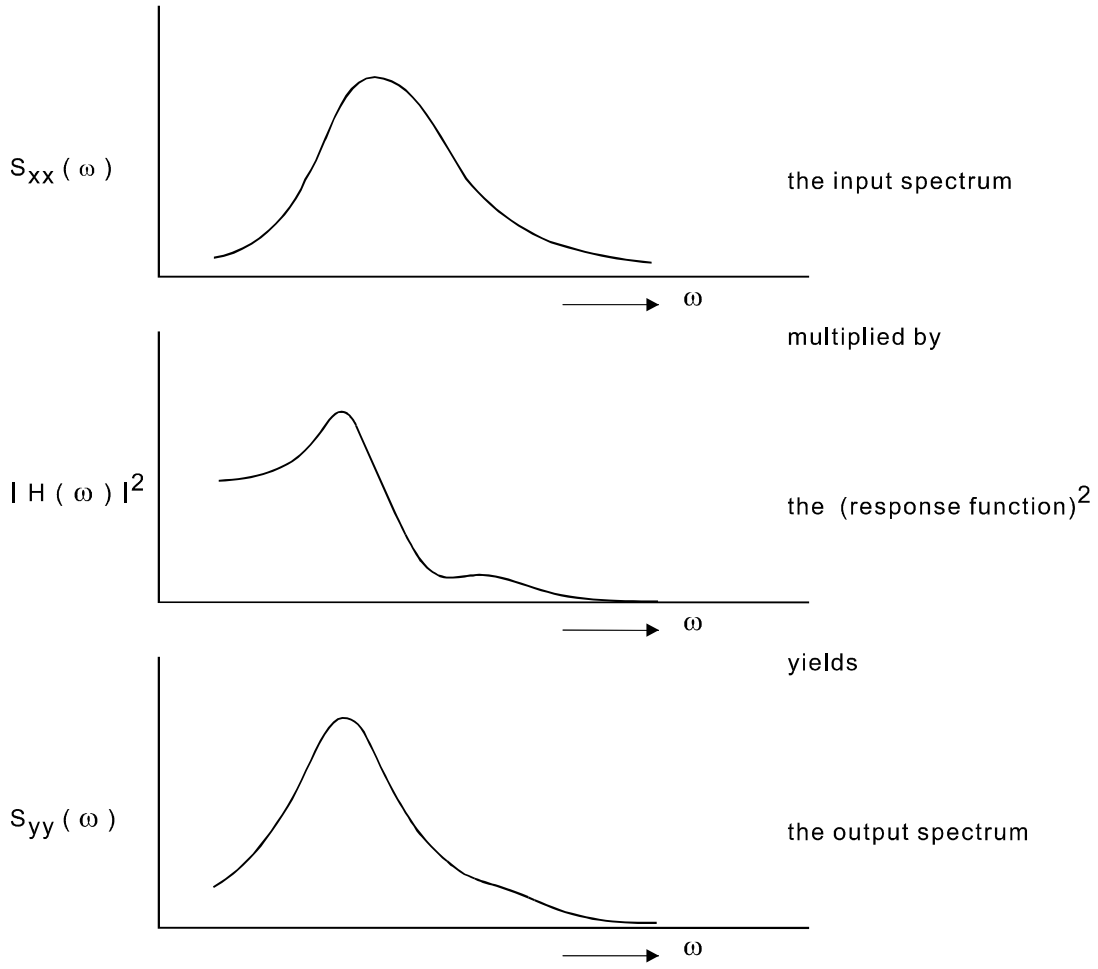

Some relations

The following quantities can now be calculated with use of the spectral density function:

$$m_{x0} = \int_0^\infty S_{xx}(\omega)\, d\omega \tag{20}$$

and

$$m_{x1} = \int_0^\infty S_{xx}(\omega)\, \omega\, d\omega \tag{21}$$

For a stochastic variable x, describing a stationary ergodic process, is:

$$\overline{M}_x = \frac{1}{2} \int_{-\infty}^{\infty} S_{xx}(\omega)\, d\omega \tag{14}$$

When $S_{xx}(\omega)$ is an even, real function and x has a narrow spectrum and zero mean value, it follows that:

$$\overline{M}_x = \int_0^\infty S_{xx}(\omega)\, d\omega = m_{x0} \quad \text{(= area under the spectrum)}$$

and:

$$\sigma_x = \sqrt{\overline{M}_x} = \sqrt{m_{x0}} \tag{22}$$

$$T_1 = 2\pi \frac{m_{x0}}{m_{x1}} \tag{23}$$

When x follows a normal distribution, then it can be calculated that:

$$4\sigma_x = 2x_{a1/3} \quad \text{(significant double amplitude)} \tag{24}$$

Irregularity of waves

Since it is known that the distributions of the wave elevations at sea are approximately normal, all formulae mentioned earlier are valid to describe irregular sea conditions. To judge the behaviour of vessels at sea, irregular seas are assumed to have energy spectral density functions - or power spectra - that can be described by:

$$S_{\zeta\zeta}(\omega) = A \,.\, \omega^{-r} \,.\, e^{-B \,.\, \omega^{-s}} \tag{25}$$

Formula (25) represents the hypothetical spectra, similar to the Pierson-Moskowitz[6)] spectra for fully developed seas when:

r = 5,
s = 4,
A = 172.8 $(\zeta_{w1/3})^2 (T_1)^{-4}$
B = 691.0 $(T_1)^{-4}$

Assuming that the wave height is a random variable with a narrow band normal distribution and zero mean value one arrives at (see also (24) and (23)):

$$\zeta_{w1/3} \simeq 4\sqrt{m_{\zeta 0}}$$

$$T_1 \simeq 2\pi \frac{m_{\zeta 0}}{m_{\zeta 1}}$$

where $\zeta_{w1/3}$ is the significant wave height and T_1 the average wave period.

In relating the spectra (25) to observations, the average observed wave height ζ_w is assumed to coincide with the significant wave height $\zeta_{w1/3}$. The average observed period T is assumed to coincide with the average calculated period T_1. So, observed sea conditions can be represented by means of a spectrum, as shown in Figure E, where the observations of H.U. Roll on the North Atlantic Ocean are represented in Pierson-Moskowitz spectra.

6) Pierson, W.J. and Moskowitz, L.; "A Proposed Spectral Form for Fully Developed Wind Seas Based on Similarity Theory of S.A. Kitaigorodskii", Journal of Geophysical Research, Vol. 69, December 1964.

Figure E

PIERSON-MOSKOWITZ SPECTRA
(s = 4) and (r = 5)
Significant wave height $\zeta_{w1/3}$ and average period T_1
according to Roll for the North Atlantic Ocean
$T_1 = 2\pi\ (m_{\zeta 0}/m_{\zeta 1})$

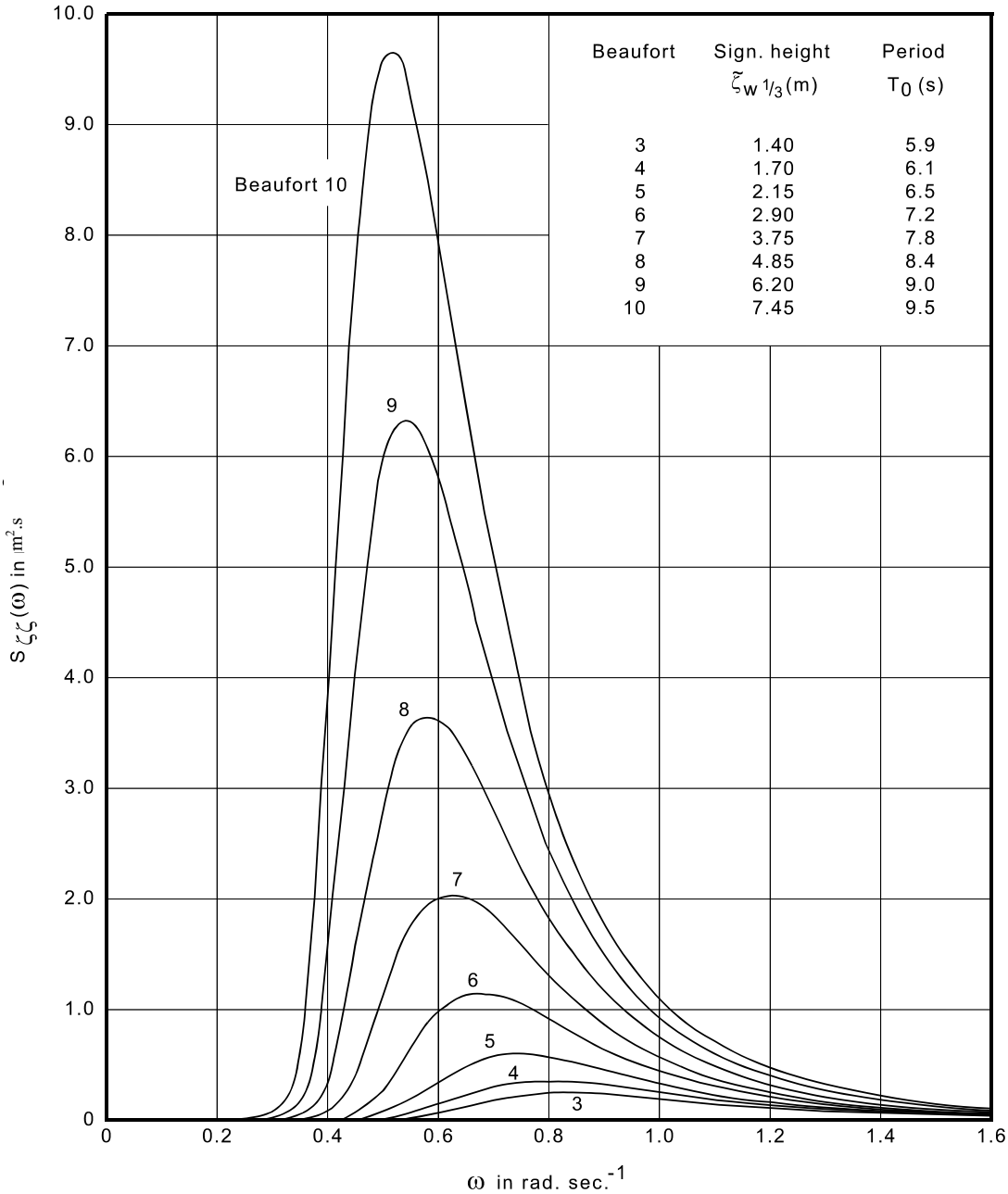

Irregularity of waves

Since it is known that the distributions of the wave elevations at sea are approximately normal, all formulae mentioned earlier are valid to describe irregular sea conditions. To judge the behaviour of vessels at sea, irregular seas are assumed to have energy spectral density functions - or power spectra - that can be described by the JONSWAP[7)] formula:

$$S_{\zeta\zeta}(\omega) = \alpha \,.\, g^2 \,.\, \omega^{-5} \,.\, \exp\left[-1.25\,(\omega/\omega_0)^{-4}\right] \,.\, \gamma^{\exp\left[-(\omega-\omega_0)^2/(2\sigma^2\,.\,\omega_0^2)\right]} \tag{26}$$

$$\sigma = \begin{cases} \sigma_a \text{ for } \omega \le \omega_0 \\ \sigma_b \text{ for } \omega > \omega_0 \end{cases}$$

in which:

ω	=	circular frequency
ω_0	=	spectral peak frequency
g	=	acceleration due to gravity

The dimensionless shape parameters α, γ, σ_a and σ_b are generally taken as:

$\alpha = 0.0989$; $\gamma = 3.3$; $\sigma_a = 0.07$; $\sigma_b = 0.09$

Assuming that the wave height is a random variable with a narrow band normal distribution and zero mean value one arrives at (see also (24) and (23)):

$$\zeta_{w1/3} \simeq 4\sqrt{m_{\zeta 0}}$$

$$T_1 \simeq 2\pi \frac{m_{\zeta 0}}{m_{\zeta 1}}$$

where $\zeta_{w1/3}$ is the significant wave height and T_1 the average wave period.

In relating the spectra (26) to observations, the average observed wave height ζ_w is assumed to coincide with the significant wave height $\zeta_{w1/3}$. The average observed period T is assumed to coincide with the average calculated period T_1. So, observed sea conditions can be represented by means of a spectrum, as shown in Figure F, for a range of Beaufort numbers.

7) Hasselman, K. et al.; "Measurement of Wind-wave Growth and Swell Decay During the Joint North Sea Wave Project (JONSWAP)", Deutsches Hydrographisches Institut Hamburg, 1973.

NOTE: The relation between the average period T_1 and the peak period T_0 for the JONSWAP type spectra is $T_0/T_1 = 1.20$.

Figure F

JONSWAP SPECTRA

Significant wave height $\zeta_{w1/3}$ and peak period T_0
according to Roll for the North Atlantic Ocean

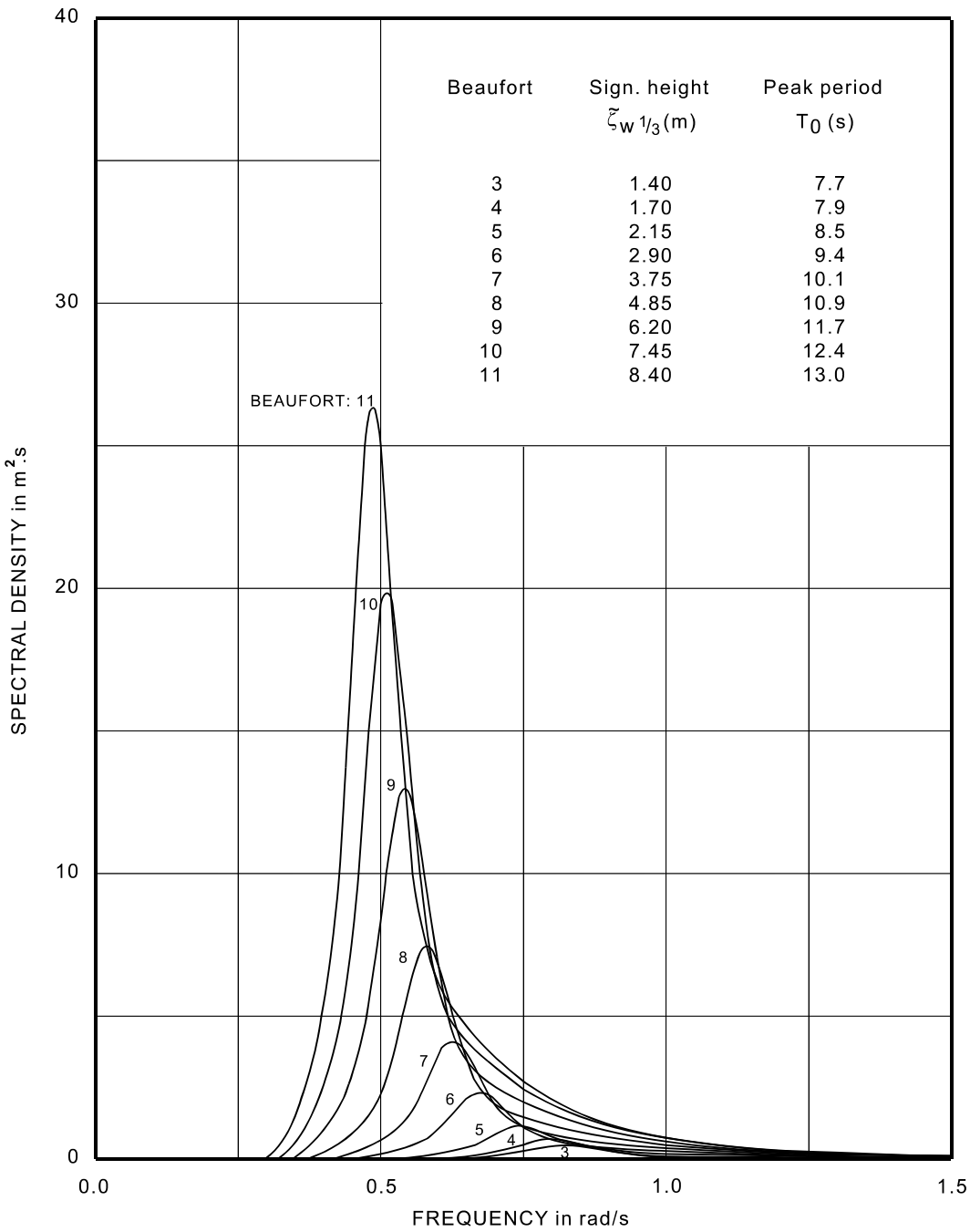

APPENDIX D03

Statistical Analysis

Revision	Date	Description of revision	Author
0	September 10, 2009	First version of the appendix.	JLC
1	February 26, 2010	Review and up-date of the text.	JLC
2	September 1, 2010	Remark on extremes in STATAN added.	JH/JJS
3	April 11, 2018	Adjusted to SHARK	JvdB

Statistical Analysis

The data analysis of the model tests or simulations includes a statistical analysis of the recorded time signals. Two types of statistical analysis are available, being "GEMBER" and "STATAN". The GEMBER tables contain a limited statistical analysis based on all samples in the signal. The STATAN tables contain a more detailed statistical analysis. The statistical quantities included in both analysis methods are listed below.

Sample based statistical analysis tables

The following quantities are determined for the measured and calculated time signals.

1. *Mean value*: $\bar{u}$ (MEAN)

   $$\bar{u} = \frac{1}{N}\sum_{n=1}^{N} u_n \quad (N = \text{number of samples})$$

2. *Standard deviation*: σ_u (ST.DEV)

   $$\sigma_u = \sqrt{\frac{1}{N}\sum_{n=1}^{N}(u_n - \bar{u})^2}$$

3. *Maximum value*: A MAX +
   Highest crest value.

4. *Maximum value*: A MAX -
   Highest trough value.

Extrema statistical analysis tables

The following quantities are determined for the measured and calculated time signals.

5. *Maximum value*: A MAX +
   Highest crest value.

6. *Maximum value*: A MAX -
   Highest trough value.

7. *Maximum double amplitude*: 2A MAX
   This is the maximum crest to trough value.

8. *Significant peak value*: A 1/3 +
   This is the mean of the highest one-third zero to crest values.

9. *Significant trough value*: A 1/3 -
   This is the mean of the highest one-third zero to trough values.

10. *Significant double amplitude*: 2A 1/3
    This is the mean of the highest one-third crest to trough values.

11. *Number of oscillations*: NO
    This is the total number of oscillations in the record.

The extrema used for the extrema statistics can be either local extrema or zero cross extrema. Before determination of the extrema, a low pass filter is usually applied to the input time trace.

APPENDIX D05

Description of the 3-Parameter Weibull Fit

Revision	Date	Description of revision	Author
0	September 10, 2009	First version of the appendix	JH
1	February 1, 2010	Review and up-date of the text	JLC

Description of the 3-Parameter Weibull Fit

The values "A MAX. +" and "A MAX. -" presented in the tables with statistical output represent the measured maximum and minimum values, as observed during the test or simulation. For design purposes, however, the so-called "most probable maximum" (MPM-) value is often applied. This is a statistically more reliable maximum value. The most probable maximum is defined as follows:

$$P\,(X > X_{MPM}) = \frac{1}{N} \cdot 100\%$$

in which:

P	=	probability of exceedance, [-]
X	=	variable, e.g. the turret motion
X_{MPM}	=	"most probable maximum" (MPM-) value for variable X
N	=	number of oscillations in duration for which the value of X_{MPM} is determined

The MPM-value is the extreme value with the probability to occur once during the duration of the storm (P = 1/N). The MPM-value, therefore, will depend on the storm duration or the number of oscillations N; a longer storm duration will lead to a higher most probable maximum. The number of oscillations N is counted for each signal and can be found in the tables with the results of the statistical.

From the test or simulation results MPM-values can be determined using the distribution of the extremes plotted on Weibull paper. Because the highest measured maximum is deleted from Weibull plots (for this value no probability of exceedance can be determined), the most probable maximum with the same probability is determined based on an extrapolation of the upper part of the curve of the Weibull plots.

The 3-parameter Weibull fit is defined as follows:

$$P(x) = e^{-\left(\frac{x-\theta}{\alpha}\right)^{\beta}}$$

in which:

P(x)	=	probability of exceedance of value x
□	=	scale parameter
□	=	shape parameter
□	=	location parameter

On Weibull paper the 3-parameter Weibull fit is a straight line.

The values of □, □ and □ are determined using a least-squares fitting procedure through the peak values obtained from the recorded signal. The calculated values for □, □ and □ can be found at the top of the Weibull plots.

The formulation on the previous page can be used to determine the probability of exceedance P for a given peak value x. Alternatively, the 3-parameter Weibull distribution can be represented as follows:

$$x(P) = \theta + \alpha \cdot \sqrt[\beta]{-\ln(P)}$$

This formulation can be used to determine the peak value for a given probability of exceedance. The MPM-value is defined as the peak value with a probability to occur once during the storm duration (or: P = 1/N). Therefore, if a 3-parameter Weibull fit is available, the MPM-value can then be calculated as follows:

$$x_{MPM} = \theta + \alpha \cdot \sqrt[\beta]{-\ln\left(\frac{1}{N}\right)} \qquad \text{for maxima}$$

$$x_{MPM} = \theta - \alpha \cdot \sqrt[\beta]{-\ln\left(\frac{1}{N}\right)} \qquad \text{for minima}$$

in which:

α,β,θ	=	Weibull fit parameters
N	=	number of peaks in the signal

The calculated MPM values are shown at the top of the Weibull plots with a fitted line. They are shown next to the calculated □, □ and □ values.

Remark

It should be noted that an MPM-value determined from the fitted line in the Weibull distribution depends on the values of the parameters □, □ and □ and may be affected by the selection of peaks used in the least-squares fit. Typically, the 25% or 50% highest peaks are included in the analysis, but the selected percentage is more or less arbitrary. In sensitive cases, it is therefore recommended to also determine the MPM-value using e.g. the highest 10%, 25%, 50% and 75% of the peaks in order to check the robustness of the determined MPM-value.

Furthermore, it must be noted that the quality of the MPM-value depends on the distribution function of the analyzed signals. Some signals show only one or two extreme peaks (very low probability of exceedance), while the rest of the peaks show a closer agreement with the distribution function. This behaviour depends on the applied wave realisation and non-linear effects. Due to the combination of a low probability of exceedence of the single peak and the Weibull fit based on the majority of the peaks the MPM-value can show a large deviation from the maximum value.

APPENDIX D06

Determination of Response Functions on basis of Cross-correlation Method

Revision	Date	Description of revision	Author
0	May 19, 2009	First version of the appendix	JLC
1	April 18, 2017	Update Jaap de Wilde	JdW

Determination of Response Functions on Basis of Cross-correlation Method

Introduction

This appendix describes the relation between two processes x(t) and y(t) being the input and output signal respectively of a physical system.

x(t) → System → y(t)

For instance: the input signal can be an irregular wave and the output signal the resulting motion of a floating structure.

It will be assumed that the signals discussed are realisations of random processes being stationary and ergodic. Stationary means that the statistical properties of the realisations are independent of time, while ergodicity indicates that one single realisation of the process determines the statistical properties of the process completely.

Characterisation of input-output system in frequency domain

For a description of the input-output system in the frequency domain use can be made of the so-called cross-spectral density function being defined as the Fourier transform of the cross-correlation function:

$$S_{xy}(\omega) = \frac{1}{\pi} \int_{0}^{+\infty} R_{xy}(\tau)\, e^{-i\omega\tau}\, d\tau \tag{2}$$

Since the cross-correlation function $R_{xy}(\tau)$ is not an even function its Fourier transform has the complex form. The cross-spectral density function consists therefore of a real and an imaginary part or an amplitude and a phase part:

$$S_{xy}(\omega) = A_{xy}(\omega) e^{-i\phi_{xy}(\omega)} \tag{3}$$

Frequency response functions

If a system with an input signal x(t) and output signal y(t) is linear, an impulse response function h(t) can be defined so that:

$$y(t) = h(t) * x(t) = \int_{-\infty}^{+\infty} h(\tau)\, x(t-\tau)\, d\tau \tag{4}$$

,where $*$ denotes a convolution.

Transformation to the frequency domain yields:

$$Y(\omega) = H(\omega)\, X(\omega) \tag{5}$$

where $X(\omega)$, $Y(\omega)$ and $H(\omega)$ are the Fourier transforms of x(t), y(t) and h(t) respectively.

The quantity $|H(\omega)|$ is called the frequency response function and $\phi_H(\omega)$ is the phase response function.

$$H(\omega) = |H(\omega)| e^{-i\phi_H(\omega)} \tag{6}$$

From (12) it can be found that:

$$|H(\omega)| = \sqrt{\frac{S_{yy}(\omega)}{S_{xx}(\omega)}} \tag{7}$$

in which $S_{xx}(\omega)$ and $S_{yy}(\omega)$ are the scalar spectra of the signals x(t) and y(t), being defined as the Fourier transform of the auto-correlation functions $R_{xx}(\tau)$ and $R_{yy}(\tau)$ respectively:

$$S_{yy} = \frac{1}{2\pi} \int_{-\infty}^{+\infty} R_{yy}(\tau) e^{-i\omega\tau} d\tau \tag{8}$$

$$S_{yy} = \frac{1}{2\pi} \int_{-\infty}^{+\infty} R_{yy}(\tau) e^{-i\omega\tau} d\tau \tag{9}$$

If both the amplitude and the phase response function are required use has to be made of the cross-spectral density functions $S_{xy}(\omega)$ and the scalar spectral density function of the input $S_{xx}(\omega)$ as is shown below:

$$\begin{aligned} R_{xy}(\tau) &= \lim_{T\to\infty} \frac{1}{2T} \int_{-T}^{T} x_r(t)\, y_r(t+\tau)\, d\tau = \\ &= \lim_{T\to\infty} \frac{1}{2T} \int_{-T}^{T} \left\{ x_r(t) \int_{-\infty}^{+\infty} h(\theta)\, x_r(t+\tau-\theta) d\theta \right\} dt = \\ &= \int_{-\infty}^{+\infty} h(\theta) R_{xx}(\tau-\theta) d\theta \end{aligned} \tag{10}$$

The Fourier transform yields:

$$\begin{aligned} S_{xy}(\omega) &= \frac{1}{2\pi} \int_{-\infty}^{+\infty} e^{-i\omega\tau} \left\{ \int_{-\infty}^{+\infty} h(\theta) R_{xx}(\tau-\theta)\, d\theta \right\} d\tau \\ &= \frac{1}{2\pi} \int_{-\infty}^{+\infty} \left\{ h(\theta) e^{-i\omega\theta} \int_{-\infty}^{+\infty} R_{xx}(\tau-\theta)\, e^{-i\omega(\tau-\theta)}\, d\tau \right\} d\theta \\ &= \left\{ \int_{-\infty}^{+\infty} h(\theta)\, e^{-i\omega\theta}\, d\theta \right\} S_{xx}(\omega) \\ &= H(\omega)\, S_{xx}(\omega) \end{aligned} \tag{11}$$

This shows that:

$$H(\omega) = \frac{S_{xy}(\omega)}{S_{xx}(\omega)} \tag{12}$$

in which $H(\omega)$ and $S_{xy}(\omega)$ have the complex form.

The amplitude response function $|H(\omega)|$ is given by:

$$|H(\omega)| = \frac{|S_{xy}(\omega)|}{S_{xx}(\omega)} = \frac{A_{xy}(\omega)}{S_{xx}(\omega)} \tag{13}$$

and the phase response function by:

$$\phi_H(\omega) = \arg\frac{S_{xy}(\omega)}{S_{xx}(\omega)} = \phi_{xy}(\omega) \tag{14}$$

In addition to the given variables the coherency function $\gamma^2_{xy}(\omega)$ can be defined as:

$$\gamma^2_{xy}(\omega) = \frac{|S_{xy}(\omega)|^2}{S_{xx}(\omega)S_{yy}(\omega)} \tag{15}$$

The coherency function is defined to be a measure for the linear dependence or the correlation between the frequency components of the two processes.

For a purely linear system the coherency function becomes unity. For completely uncorrelated input and output processes the coherency function becomes zero.

Usually the coherency will be between these two extremes:

$$0 \le \gamma^2_{xy}(\omega) \le 1 \tag{16}$$

due to one or more of the following reasons:

- insufficient accurate spectral estimates for S_{xx}, S_{yy} and S_{xy};
- the presence of noise in either one or both of the records;
- non-linear effects.

In summary we have seen that the amplitude response function can be obtained in two different ways, respectively:

$$|H(\omega)|_{(1)} = \sqrt{\frac{S_{yy}(\omega)}{S_{xx}(\omega)}}$$

and

$$|H(\omega)|_{(2)} = \frac{|S_{xy}(\omega)|}{S_{xx}(\omega)}$$

References

[1] Newland, D.E.; “An Introduction to Random Vibrations and Spectral Analysis”, Longman Scientific & Technical, Second edition, 1984.

APPENDIX D12

Calculation of Derived Quantities

Revision	Date	Description of revision	Author
0	June 22, 2015	First version of the appendix	FJ
1	July 23, 2015	Description of force frame added	FJ
2	October 4, 2017	Derived Quantities of Wind Calibration Added	AN
3	November 16, 2018	Several improvements & additions	AN

Calculation of Derived Quantities

This appendix describes how the derived quantities are calculated from the signals measured in the basin. The description of the following derived quantities are included in this Appendix:

- Loads and moments at different fender locations
- Motions of different modules

LOADS AND MOMENTS AT DIFFERENT FENDER LOCATIONS

Calculation of loads and moments at heart fenders between:

- ***Modules L1 and L7 (Frames L1-1 to L1-4)***
- ***Modules M1 and L12 (Frames L121 and L122)***
- ***Modules M2 and L12 (Frames L123 and L124)***

For the model tests, force transducer frames were mounted between modules L1 and L7, between modules M1 and L12 and between modules M2 and L12. These frames are used to calculate the forces and moments at the fender locations located nearby these frames. Six force transducers are installed in such a frame to measure the loads in the six-degrees of freedom.

The following formulas are used to calculate the forces and moments around the different fenders at those locations:

Fx = FxCLU + FxPSL + FxSBL
Fy = FY
Fz = FzPS + FzSB
Mx = (FzPS – FzSB) . 3.27
My = (FxCLU – FxPSL – FxSBL) . 1.86 – (FzPS +FzSB) . 5.31
Mz = (FxSBL – FxPSL) . 1.98 +FY . 5.31

in which:

Fx	[kN]	:	Longitudinal force
Fy	[kN]	:	Transverse force
Fz	[kN]	:	Vertical force
Mx	[kNm]	:	Moment about the x-axis at centre of fender
My	[kNm]	:	Moment about the y-axis at centre of fender
Mz	[kNm]	:	Moment about the z-axis at centre of fender
FxCLU	[kN]	:	Measured longitudinal force centre line up
FxPSL	[kN]	:	Measured longitudinal force port side bottom
FxSBL	[kN]	:	Measured longitudinal force starboard bottom
FY	[kN]	:	Measured transverse force
FzPS	[kN]	:	Measured vertical force port side
FzSB	[kN]	:	Measured vertical force starboard

Calculation of loads and moments at heart fenders between:

- ***Modules L1 and L2 (Frames L2-1 to L2-2)***

For the model tests, force transducer frames were mounted between modules L1 and L2. These frames are used to calculate the forces and moments at the fender locations located nearby these frames. Six force transducers are installed in such a frame to measure the loads in the six-degrees of freedom.

The following formulas are used to calculate the forces and moments around the different fenders at those locations:

Fx = FX
Fy = FyCLU + FyFL + FyAL
Fz = FzF + FzA
Mx = (FyFL + FyAL – FyCLU) . 1.86 – (FzF + FzA) . 5.31
My = (FzA – FzF) . 3.27
Mz = FX . 5.31 + (FyFL – FyAL) . 1.98

in which:

Fx	[kN]	:	Longitudinal force
Fy	[kN]	:	Transverse force
Fz	[kN]	:	Vertical force
Mx	[kNm]	:	Moment about the x-axis at centre of fender
My	[kNm]	:	Moment about the y-axis at centre of fender
Mz	[kNm]	:	Moment about the z-axis at centre of fender
Fx	[kN]	:	Measured longitudinal force
FyCLU	[kN]	:	Measured transverse force centre line up
FyFL	[kN]	:	Measured transverse force fore bottom
FyAL	[kN]	:	Measured transverse force aft bottom
FzF	[kN]	:	Measured vertical force fore
FzA	[kN]	:	Measured vertical force aft

MOTIONS OF DIFFERENT MODULES

Earth fixed motions of different modules

During the tests the motions of the measuring target of different modules were measured. The location of the targets during the model test programme is listed in TABLE 3. For each instrumented module the motion at the CoG of the module has been calculated. For the calculation of the earth-fixed motions at a point P (e.g. the centre of gravity) from the measured motions the formulas below were used.

$$\begin{pmatrix} x_e \\ y_e \\ z_e \end{pmatrix} = \begin{pmatrix} x_{meas} \\ y_{meas} \\ z_{meas} \end{pmatrix} + \begin{pmatrix} D_{11} & D_{12} & D_{13} \\ D_{21} & D_{22} & D_{23} \\ D_{31} & D_{32} & D_{33} \end{pmatrix} \cdot \begin{pmatrix} A \\ B \\ C \end{pmatrix}$$

in which:

x_{meas}	=	measured X-translation of measurement point in earth fixed system
y_{meas}	=	measured Y-translation of measurement point in earth fixed system
z_{meas}	=	measured Z-translation of measurement point in earth fixed system
□	=	measured roll motions
□	=	measured pitch motions
□	=	measured yaw motions
A	=	ship fixed X-co-ordinate of point P from measurement point
B	=	ship fixed Y-co-ordinate of point P from measurement point
C	=	ship fixed Z-co-ordinate of point P from measurement point

and

$$D_{11} = \cos(\psi)\cdot\cos(\theta)$$
$$D_{12} = -\sin(\psi)\cdot\cos(\varphi) + \cos(\psi)\cdot\sin(\theta)\cdot\sin(\varphi)$$
$$D_{13} = \sin(\psi)\cdot\sin(\varphi) + \cos(\varphi)\cdot\cos(\psi)\cdot\sin(\theta)$$

$$D_{21} = \sin(\psi)\cdot\cos(\theta)$$
$$D_{22} = \cos(\psi)\cdot\cos(\varphi) + \sin(\psi)\cdot\sin(\theta)\cdot\sin(\varphi)$$
$$D_{23} = -\cos(\psi)\cdot\sin(\varphi) + \cos(\varphi)\cdot\sin(\psi)\cdot\sin(\theta)$$

$$D_{31} = -\sin(\theta)$$
$$D_{32} = \cos(\theta)\cdot\sin(\varphi)$$
$$D_{33} = \cos(\theta)\cdot\cos(\varphi) - 1$$

In this way the motions at several locations as listed in TABLE 7 were calculated.

APPENDIX E01

Description of the Offshore Basin wind, wave and current generation systems

Revision	Date	Description of revision	Author
0	May 27, 2009	First version of the appendix	JH

Description of the Offshore Basin wind, wave and current generation systems

The model tests in combined environments will be carried out in MARIN's Offshore Basin (OB). This basin offers a number of unique possibilities for the modelling of current, waves and wind.

The figure below shows a cross section of the Offshore Basin.

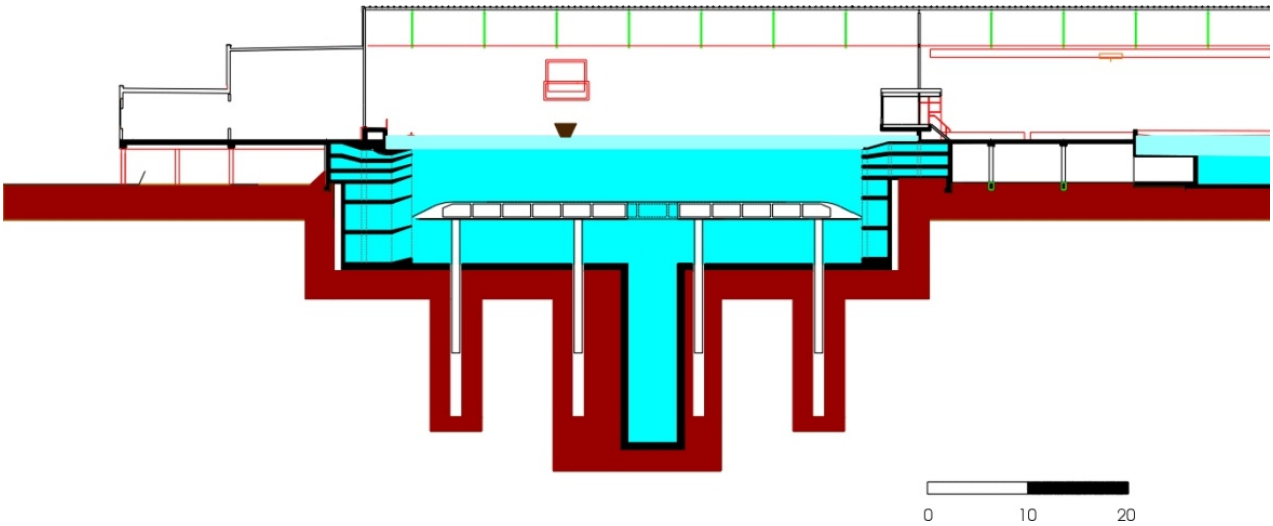

The basin measures 46 m * 36 m and has a movable floor (dimensions 36.35 m * 31.6 m), which is used to adjust the water depth. The maximum water depth measures 10.2 m at model scale. The basin also has a deep pit, with a maximum depth of 30 m.

The current generation system consists of 6 separate layers, each equipped with its own pump. Current can be generated over the full depth of 10.2 m. The water is re-circulated through a system of channels outside the basin, in order to avoid re-circulation in the basin itself. This current generation system enables the adjustment of vertical current profiles. The picture below shows a cross section of the 6 current layers at the current inflow openings into the basin.

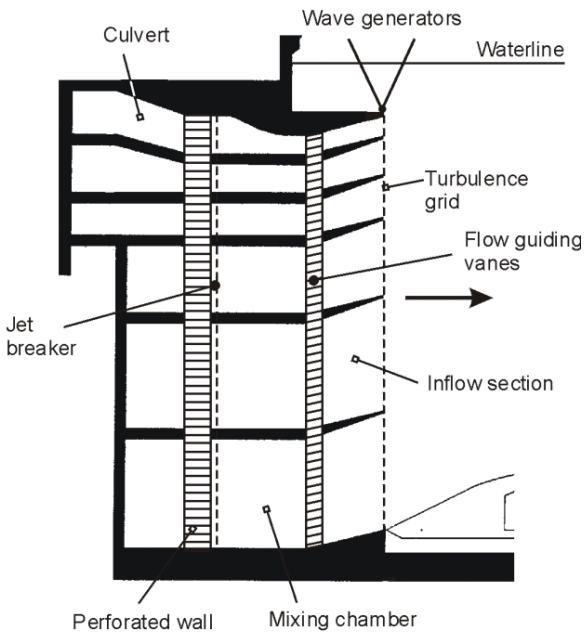

The uppermost layer is directly located under the 1.2 m high wave generators. The uniformity of the flow in the basin is obtained by flow distributing in- and outflow culverts.
To measure and adjust vertical current profiles, an electro-magnetic speed (EMS) probe mounted on a vertical traversing system is used. The EMS probe is an ellipsoidal probe for high spatial resolution and minimum disturbance. It is able to measure biaxial current velocities. Two types of measurements are carried out:

- Sweep measurements with a small constant vertical velocity of the probe to determine the vertical profile
- Stationary measurements a certain depths to determine the behaviour of the current in time (turbulence levels).

The figure below shows an example of a modelled vertical current profile. A sweep measurement was taken (low velocity carriage travelling along tension leg type vertical support wires) as well as stationary measurements at 4 depths.

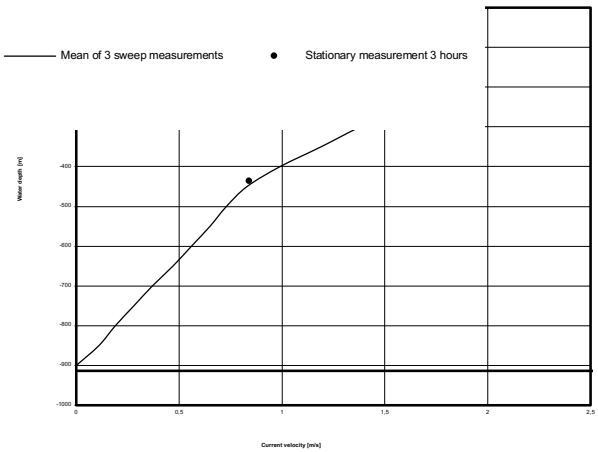

The next figure shows the time traces of the 4 stationary measurement points: 2 in the upper constant part, 2 in the sheared current part.

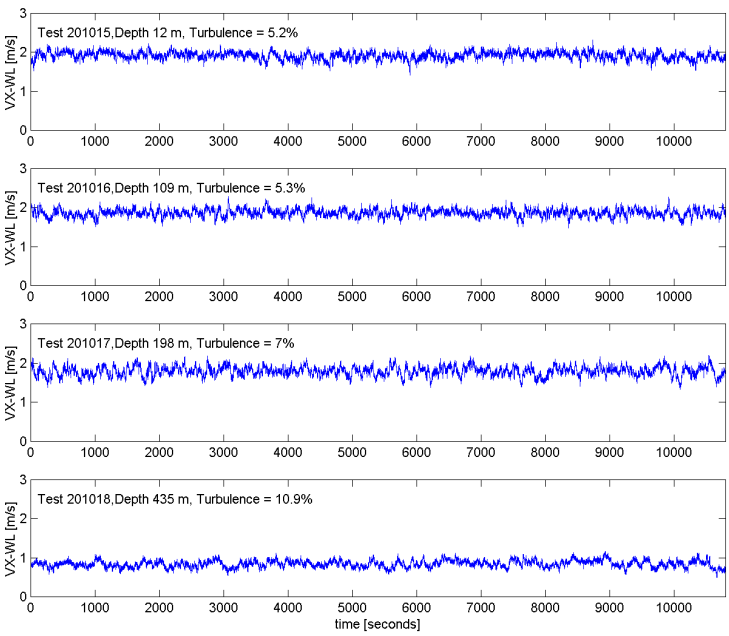

In the constant upper part the variation is very low (Turbulence level=5%), in the sheared current the variation is slightly higher (Turbulence level=7% and 10.9%) but this is a result of the natural processes in sheared current. For the present project it is recommended to keep the current constant over the entire low depth. A constant current guarantees the modelling of a realistic current load and a correct wave-current interaction.

Irregular waves are generated by a system of approximately 200 oscillating flaps. The wave flaps are shown in the picture below, showing an overview of the Offshore Basin. Each of these wave flaps is controlled individually with full control over stroke and period. This wave generation system can generate long-crested irregular seas, irregular seas with directional spreading and combinations of irregular waves and swell, each with their own direction of propagation. Wave absorbing beaches are present opposite to the wave generators.

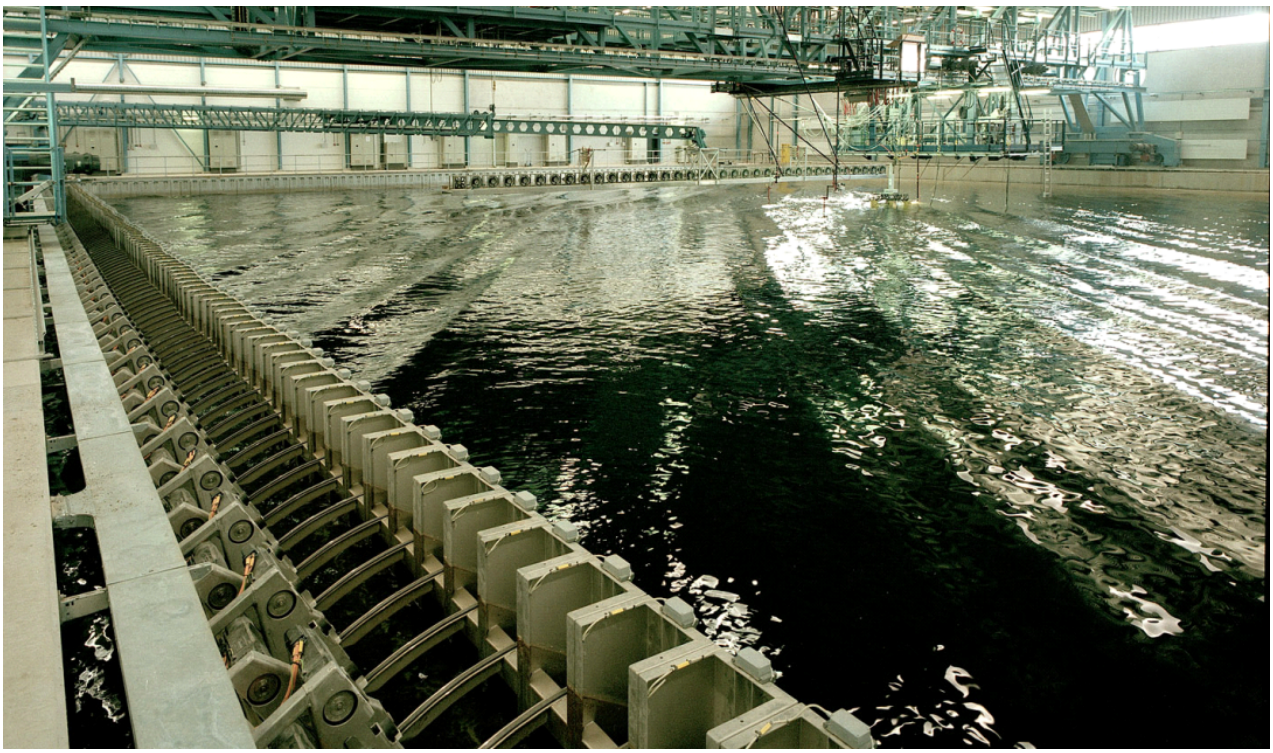

The movable floor is curved on its sides so optimize the current inflow. However, at the sides this means that the waves start to diffract in shallow water due to the difference in depth, rotating them onto the basin floor under the wrong angle. Therefore, we do not use the wave flaps in the corners anymore. The consequence is that we can only make waves perpendicular to the wave generators on both sides: either parallel with the current or perpendicular to the current.

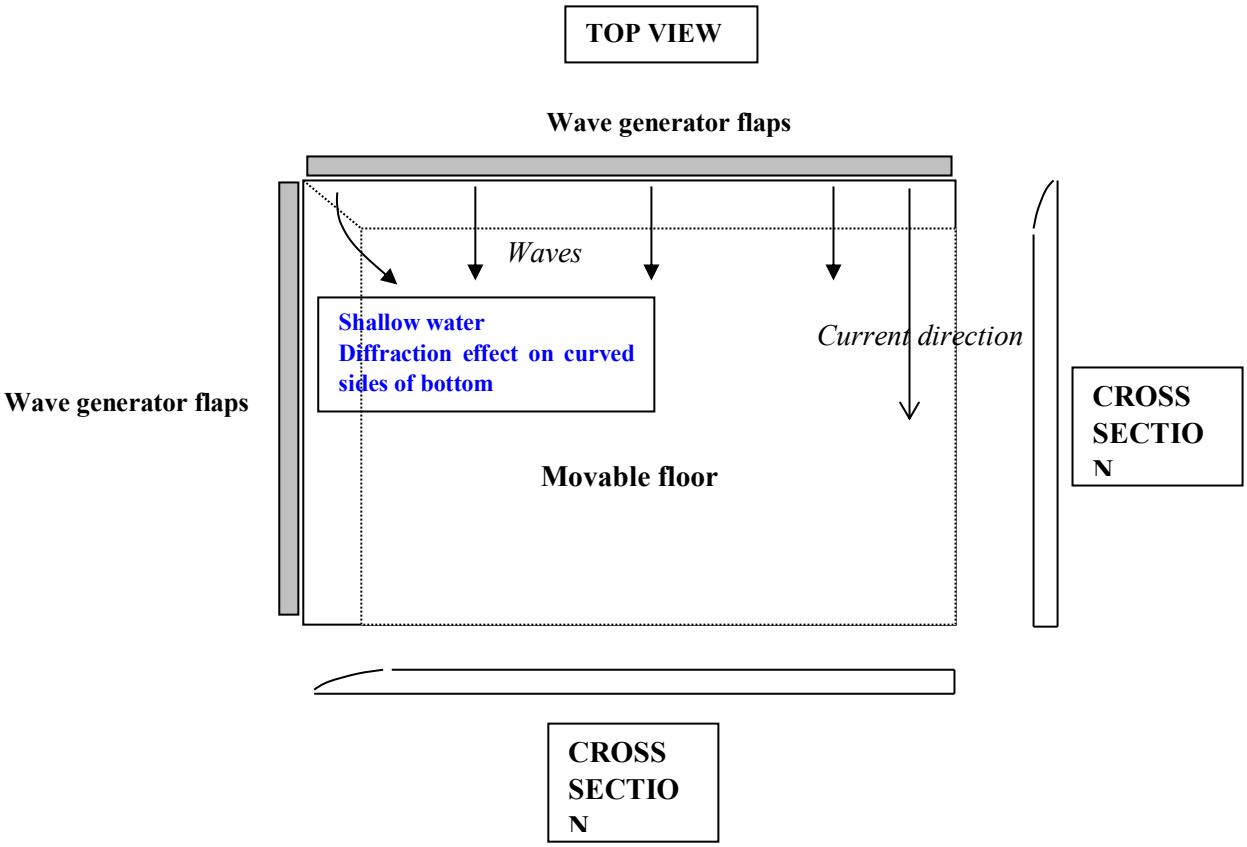

The relative angles of wind, waves and current as requested can be simulated, as shown in the figure below:

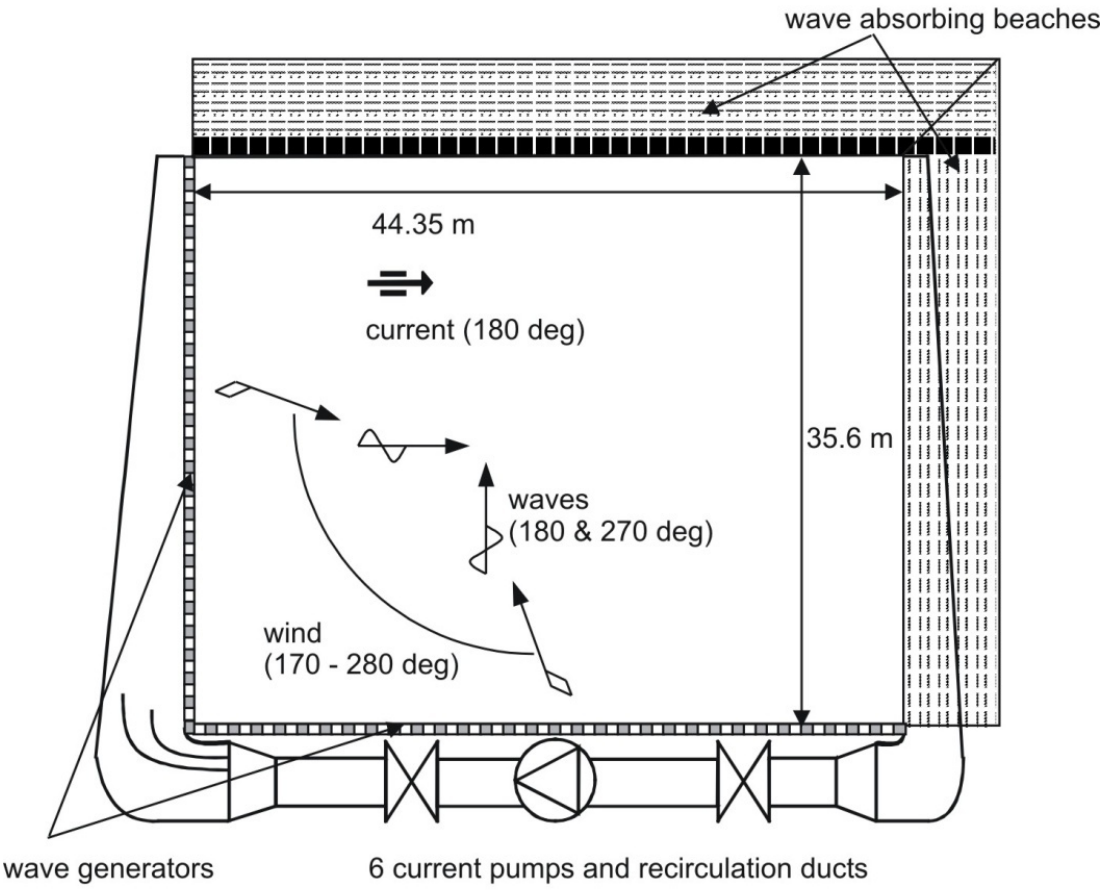

APPENDIX E02

Current Calibration Procedure in the Offshore Basin (OB)

Revision	Date	Description of revision	Author
0	May 27, 2009	First version of the appendix	Jh
1	January 31, 2010	Review and up-date of the text	Jlc

Current Calibration Procedure in the Offshore Basin (OB)

The current velocity is scaled according to Froude scaling, in order to model the correct wave-current interactions. Prior to the wave adjustments and without the model present in the basin the appropriate vertical current profile is adjusted in the basin over the basin depth. The applied current profile calibration and measurement procedure is as follows.

1. Based on the required current velocity profile the flow rate (pump RPMs) for each of the 6 current pumps is selected. The pumps are started and after the current has become stable, current velocity measurements are carried out.

2. The current velocity profile is measured by moving a current velocity probe from the basin bottom to the water surface, meanwhile measuring the velocity and the probe position. The current velocity profile is made by plotting the probe position against the measured velocity.

3. If necessary the current pump RPMs are adjusted and the measurements are repeated, until the specified current velocity profile is obtained.

4. After adjustment of the vertical current profile stationary measurements with a duration of 1 hour (proto-type value) are carried out. The purpose of these measurements is to investigate in more detail the statistical properties of the current velocity at particular depths (e.g. half the vessel draft).

5. Based on the measured time record of the current velocity from the stationary measurement a statistical analysis is performed. The turbulence level is defined as the ratio between the standard deviation and the mean value of the current velocity.

APPENDIX E03

Wave Spectrum Formulations

Revision	Date	Description of revision	Author
0	May 19, 2009	First version of the appendix	JLC

Wave Spectrum Formulations

In this appendix the mathematical formulation of a number of wave spectra used in offshore model testing is presented. Descriptions of the following spectra are included:

1. Pierson Moskowitz wave spectrum
2. JONSWAP wave spectrum
3. TMA wave spectrum
4. Gaussian spectrum
5. Ochi-Hubble wave spectrum
6. White noise spectrum
7. Some remarks on wave and group spectra

The spectral formulations are described based on the wave period and the significant wave height. In order to define the spectra $S_\zeta(\omega)$, the following definitions are required.

$H_s = 4\sqrt{m_0}$ = Significant wave height, [m]

$m_0 = \int_0^\infty S_\zeta(\omega)\cdot d\omega$ = Area under the wave spectrum or zeroth moment, [m^2]

$\omega_p = \frac{2\pi}{T_p}$ = Frequency at which the maximum energy is found, [rad/s]

T_p = Peak period, [s]

$T_1 = 2\pi\cdot\frac{m_0}{m_1}$ = Mean wave period or first period, [s]

$T_2 = 2\pi\cdot\sqrt{\frac{m_0}{m_2}}$ = Mean zero-upcrossing wave period or second period, [s]

$m_1 = \int_0^\infty \omega\cdot S_\zeta(\omega)\cdot d\omega$ = First moment, [m^2/s]

$m_2 = \int_0^\infty \omega^2\cdot S_\zeta(\omega)\cdot d\omega$ = Second moment, [m^2/s^2]

The bandwidth of a spectrum influences the time intervals between wave crests:

$$T_m = 2\pi\sqrt{\frac{m_2}{m_4}}$$ (Rice; 1944, 1945)

T_m is the mean period between wave crests. The ratio T_m/T_2 is related to the width of the spectrum. For each of the spectra the relationships between T_p, T_1 and T_2 are stated in a table in this appendix.

Pierson-Moskowitz wave spectrum (1964)

Among the wave spectra the Pierson-Moskowitz spectrum [1] is the most frequently applied one for fully developed seas. Pierson and Moskowitz have derived the wave spectral formulation for fully developed seas from analysis of wave spectra measured on the North Atlantic Ocean:

$$S_\zeta(\omega)/(H_{1/3})^2 \cdot T_1 = \frac{172.8}{(T_1 \cdot \omega)^5} \cdot e^{-\frac{691}{(T_1 \cdot \omega)^4}}$$

$$S_\zeta(\omega)/(H_{1/3})^2 \cdot T_2 = \frac{124}{(T_2 \cdot \omega)^5} \cdot e^{-\frac{496}{(T_2 \cdot \omega)^4}}$$

By means of numerical integration the following relationships between various wave periods valid for the Pierson-Moskowitz spectrum can be derived, see the table below:

Example: $T_2 = 0.71\ T_p$		T_1	T_p	T_2
Average wave period	$T_1 =$	1	0.77	1.086
Period of the spectral component associated with maximum wave energy (peak period)	$T_p =$	1.296	1	1.408
Mean zero-upcrossing period	$T_2 =$	0.92	0.71	1

According to Reference [2] the following relationship between various wave heights exist for fully developed seas:

Example: $H_{1/10} = 1.27\ H_{1/3}$	$H_{1/1}$	$H_{1/3}$	$H_{1/10}$
Average wave height $H_{1/1}$	1	0.63	0.49
Significant wave height $H_{1/3}$	1.59	1	0.78
$H_{1/10}$	2.03	1.27	1

Here, $H_{1/n}$ is the mean of the wave height of the nth highest part of the wave height distribution.

JONSWAP wave spectrum (1973)

An extensive wave measurement program known as the Joint North Sea Wave Project (JONSWAP) was carried out in 1968 and 1969 along a line extending over 100 miles (160 km) into the North Sea from Silt Island. From the analysis of the measured spectra, a JONSWAP wave spectral formulation was derived which is representative of wind- generated seas with a fetch limitation, see Reference [3].

The JONSWAP spectrum, based on a period and the significant wave height, can be expressed using the formulation below. This formulation is based on a Pierson-Moskowitz type spectrum, with a "peak enhancement" factor to modify its shape.

$$S_\zeta(\omega) = \alpha \cdot g^2 \cdot \omega^{-5} \cdot \exp\left[-1.25\,(\omega/\omega_0)^{-4}\right] \cdot \gamma^{\exp\left[-(\omega-\omega_0)^2/(2\sigma^2\cdot\omega_0^{\,2})\right]}$$

$$\sigma = \begin{bmatrix} \sigma_a \text{ for } \omega \le \omega_0 \\ \sigma_b \text{ for } \omega > \omega_0 \end{bmatrix}$$

in which:

$S_\zeta(\omega)$	=	spectral density at wave frequency ω, [m^2s]
ω	=	wave frequency, [rad/s]
ω_0	=	spectrum peak frequency, [rad/s]
g	=	gravitational acceleration, [m/s^2], g = 9.81 m/s^2

A definition sketch of the parameters for the description of the JONSWAP spectrum is given in the figure below:

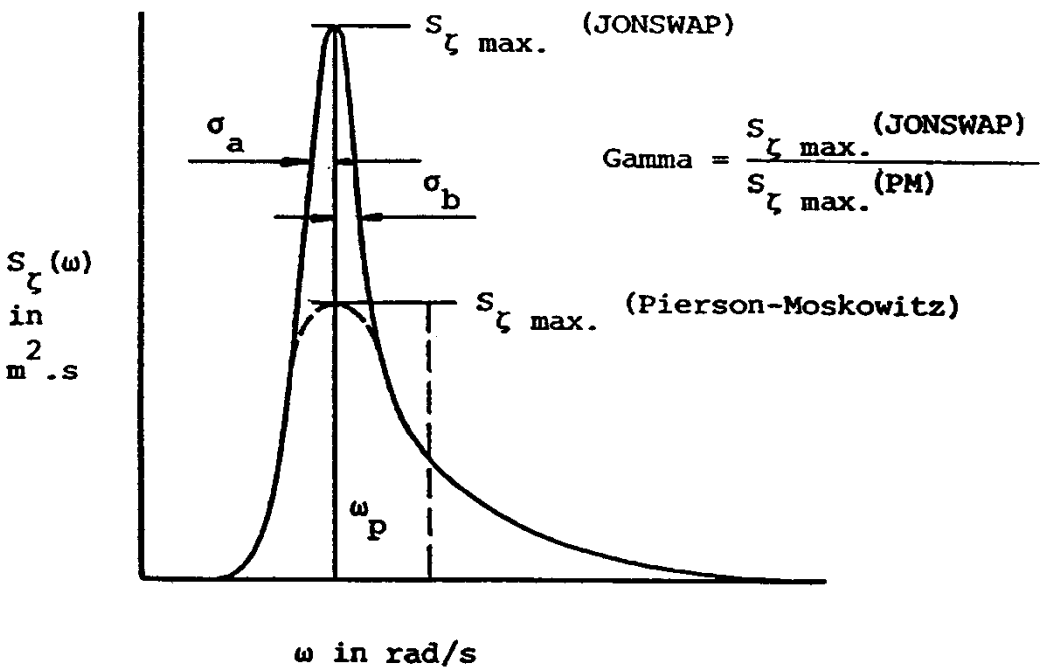

For the mean JONSWAP spectrum the authors of Reference [3] found the following values for the dimensionless spectral shape parameters σ_a, σ_b and γ.

γ	=	3.0
σ_a	=	0.07
σ_b	=	0.09

In the case that only the significant wave height $H_{1/3}$ and the average period T_1 are known, the following procedure can be applied when using the JONSWAP spectrum:

- For the shape parameters σ_a and σ_b the default values are selected (see above).
- By means of numerical integration the following relation between T_p, T_1, T_2 for the JONSWAP spectra ($\sigma_a = 0.07$ and $\sigma_b = 0.09$) as a function of γ-value was established.

γ	T_p/T_1	T_p/T_2	T_1/T_2
1.0 (P.M.)	1.296	1.408	1.086
2.0	1.240	1.338	1.079
3.0	1.206	1.295	1.073
3.3 (mean)	1.198	1.285	1.072
4.0	1.183	1.264	1.069
5.0	1.165	1.240	1.065
6.0	1.151	1.221	1.061

Using the appropriate value from the table above at a chosen γ-value in combination with the given average wave period T_1 the period of the spectral component associated with the maximum energy T_p can be calculated.

- Finally, the factor α is chosen such, that the following relation is fulfilled.

$$H_{1/3} = 4\sqrt{\int_0^\infty S_\zeta(\omega)\cdot d\omega} = 4\sqrt{m_{\zeta 0}}$$

in which:

$H_{1/3}$ = significant wave height, [m]
$m_{\square 0}$ = area beneath the wave spectrum, [m^2]

TMA wave spectrum

In shallow water conditions, instead of the JONSWAP spectrum the so-called TMA spectrum can be applied. "TMA" is an abbreviation for "Texel-Marsen-Arsloe". It is a JONSWAP spectrum modified by a term accounting for the actual water depth, see Reference [6]:

$$S_{TMA}(\omega) = S_J(\omega)\cdot\phi(\omega)$$

$$\phi(\omega) = \frac{\omega^5 \frac{\partial k}{\partial \omega}}{2g^2k^3}$$

$$\omega^2 = gk\tanh(kd);\ \frac{\partial k}{\partial \omega} = \frac{2\omega}{\frac{\omega^2}{k} + \frac{gkd}{\cosh^2(kd)}}$$

where

$S_J(\omega)$ = JONSWAP spectral density as given above at wave frequency □, [m^2s]
$\phi(\omega)$ = depth function at wave frequency □, [-]
ω = wave frequency, [rad/s]
k = wave number, [rad/m]
g = gravitational acceleration, [m/s^2], g = 9.81 m/s^2
d = water depth, [m]

Comparing TMA and JONSWAP spectra for the same significant wave height, peak period, peak enhancement factor and shape parameters, in the TMA spectrum energy is shifted to higher frequencies, see figure below for 20 m water depth:

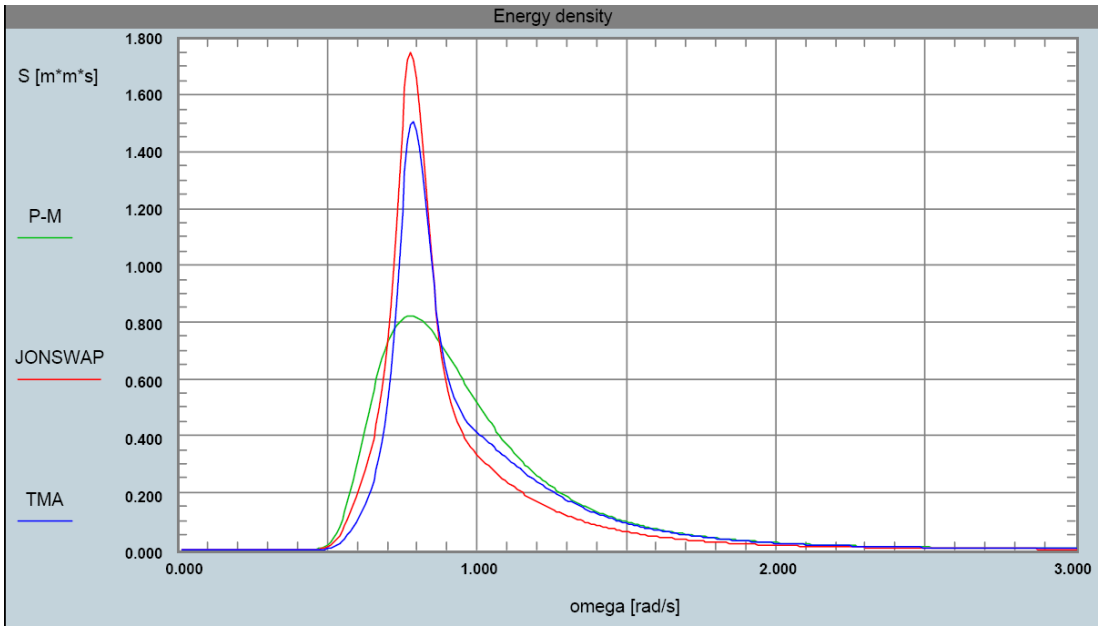

Gaussian swell spectrum

The Gaussian distribution function can be used to describe the spectrum of a swell wave. In this case, the spectral formulation is as follows:

$$S_\zeta(\omega) = \left(\frac{H_{1/3}}{4}\right)^2 \cdot \frac{1}{\sigma \cdot \sqrt{2\pi} \cdot \omega_0} \cdot \exp\left[-\frac{(\omega - \omega_0)^2}{2 \cdot \sigma^2 \cdot \omega_0^2}\right]$$

in which:

ω_0 = Spectrum peak frequency, [rad/sec]
σ = Dimensionless shape parameter, [-]
$H_{1/3}$ = Significant wave height, [m]

The Gaussian spectrum is symmetrical and therefore $T_0 = T_1 = T_2 = T_p$.

Ochi-Hubble wave spectrum

The Ochi-Hubble wave spectrum has two peaks, representing a long-period swell and short-period wind seas. The parameters defining the Ochi-Hubble wave spectrum include two values for the significant wave height H_s (one for the swell and one for the wind seas), two values for the peak period T_p (same) and two values for an enhancement factor □ (same).

The Ochi-Hubble wave spectrum can be formulated as follows:

$$S_\zeta(\omega) = \frac{1}{4} \cdot \sum_{j=1}^{2} \frac{\left[\left(4\lambda_j+1\right)\omega_{p,j}^4/4\right]^{\lambda_j}}{\Gamma(\lambda_j)} \cdot \frac{H_{s,j}^2}{\omega^{\left(4\lambda_j+1\right)}} \cdot \exp\left[-\left(\frac{4\lambda_j+1}{4}\right)\left(\frac{\omega_{p,j}}{\omega}\right)^4\right]$$

in which:

j	=	Wave component index [-], j=1 (swell), j = 2 (sea)
$H_{s,j}$	=	Significant wave height of wave component j, [m]
$\omega_{p,j}$	=	Spectrum peak frequency, [rad/sec]
$\square_j$	=	Dimensionless shape parameter, [-]
$\square$	=	Gamma function, [-]

White noise spectrum

The white noise spectrum has a constant energy distribution over a range of wave frequencies. This spectrum can be formulated as follows:

$$S_\zeta(\omega) = \begin{cases} 0 & \text{for } \omega \le \omega_b \\ \dfrac{(H_{1/3}/4)^2}{(\omega_e - \omega_b)} & \text{for } \omega_b < \omega \le \omega_e \\ 0 & \text{for } \omega > \omega_e \end{cases}$$

in which:

ω_b	=	Lowest wave frequency, [rad/sec]
ω_e	=	Highest wave frequency, [rad/sec]

Some remarks on wave and wave group spectra

In the foregoing the different wave spectrum formulations are reviewed. The wave spectral components of the spectrum will cause, according to the linear theory, the wave exciting forces and moments on the moored vessel and mooring system inducing the wave frequency motions and forces in the mooring system. The spectral shape involved, however, will not only affect the high frequency behaviour of the system. In Reference [4] it is shown that from the normal wave spectrum $S_\zeta(\omega)$ the spectrum of the square of the wave envelope can be derived theoretically. This feature is important because of the analogy which exists between the low frequency wave drifting forces and the low frequency part of the square of the heights of the incident waves, see Reference [5].

The wave elevation is written as:

$$\begin{aligned}\zeta(t) &= \sum_{i=1}^{2} \zeta_i \sin(\omega_1 t + \varepsilon_1) \\ &= \zeta_1 \sin(\omega_1 t + \varepsilon_1) + \zeta_2 \sin(\omega_2 t + \varepsilon_2)\end{aligned}$$

For small differences between ω_1 and ω_2 a schematic representation of the wave train is shown in the figure below. Such a wave train will be called a regular wave group. This type of wave train is characterized by a periodic variation of the wave envelope. The frequency associated with the envelope is equal to $\mu = \omega_2 - \omega_1$ being the difference frequency of the regular wave components.

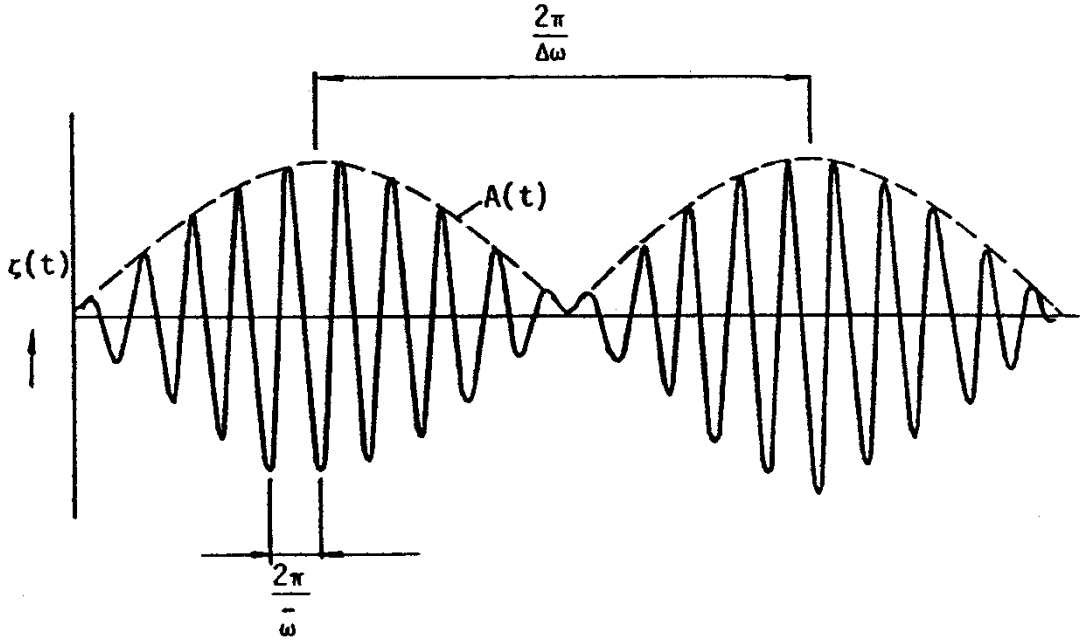

The wave elevation in amplitude modulated form can be written as:

$$\zeta(t) = A(t)\sin(\bar{\omega}t + \bar{\varepsilon})$$

in which:

$$\bar{\omega} = (\omega_1 + \omega_2)/2$$
$$\bar{\varepsilon} = (\varepsilon_1 + \varepsilon_2)/2$$

It can be shown that the envelope becomes:

$$A(t) = \left[\sum_{i=1}^{2}\sum_{i=1}^{2} \zeta_1\zeta_j \cos\left((\omega_i - \omega_j)t + (\varepsilon_i - \varepsilon_j)\right)\right]^{1/2}$$

The square of the envelope is:

$$A^2(t) = \sum_{i=1}^{2}\sum_{i=1}^{2} \zeta_1\zeta_j \cos\left((\omega_i - \omega_j)t + (\varepsilon_i - \varepsilon_j)\right)$$

or

$$A^2(t) = \zeta_1^2 + \zeta_2^2 + 2\zeta_1\zeta_2 \cos \mu t$$

in which: $\mu = \omega_2 - \omega_1$

Note that (see figure below):

$\zeta_1 = 1/2\ A^2$ in which: ζ_1 = low frequency part of the squared wave height $\zeta(t)$.

In accordance with the definition of a spectrum the spectral densities are:

$S_\zeta(\omega)\, d\omega \quad = \quad 1/2\ \zeta_a^2$

$S_{A2}(\mu)\, d\omega \quad = \quad 1/2\ p^2$ in which $p = A^2$

In accordance with the definition of a spectrum the spectral densities of the square of the wave envelope will be:

$S_{A2}(\mu)\, d\omega = 1/2\, (2\zeta_1(\omega_1)\, \zeta_2(\omega_1 + \mu))^2$

which will yield for the regular wave group with $\zeta(\omega_1)$ and $\zeta_2(\omega_2)$:

$$S_{A2}(\mu)\, d\omega = 2\, (\zeta_1(\omega_1)\, \zeta_2(\omega_1 + \mu))^2$$
$$= 2\{2\, S_{\zeta 1}(\omega_1)\, d\omega\; 2\, S_{\zeta 2}(\omega_1 + \mu)\, d\omega\}$$

or for all the wave groups with the frequency-difference μ in a wave spectrum:

$$S_{A2}(\mu) = 8 \int_0^\infty S_\zeta(\omega)\, S_\zeta(\omega + \mu)\, d\omega$$

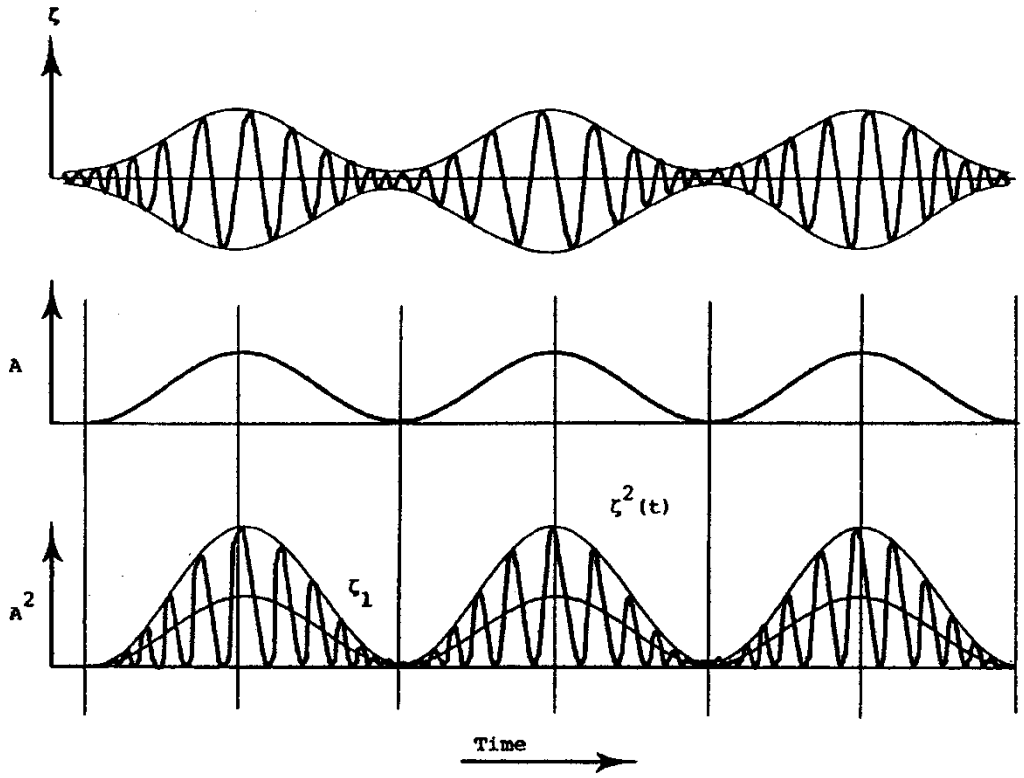

The distribution function of $A^2(t)$ is, for a narrow band spectrum:

$$P(A^2) = \frac{1}{2m_0} \cdot e^{-\frac{A^2}{2m_0}}$$

where:

$$m_0 = \int_0^\infty S_\zeta(\omega) \cdot d\omega$$

From the above, it follows that knowledge of $S_\zeta(\omega)$ and the assumption that the wave elevation is normally distributed is sufficient to calculate the spectral density and distribution function $A^2(t)$.

From the foregoing it follows that the spectral density and distribution may also be calculated from the low frequency part of the square of the record of the wave height measured in the basin. If the waves are completely random then the spectral density and distribution obtained from and based on the normal (first) spectrum of the waves should correspond with the spectral density and distribution of $2.\zeta_1^2$ calculated directly from the wave record.

The distribution function $P(A^2)$ and $p(2.\zeta_1^2)$ and the spectral density of the waves and of A^2 and $2.\zeta_1^2$ are shown in Figures A and B on the next page, respectively for an irregular wave train generated in a basin of MARIN.

As mentioned, the wave envelope is related to the low-pass filtered square of the wave elevation:

$$A(t) = \sqrt{2 \cdot \zeta_1^2(t)}$$

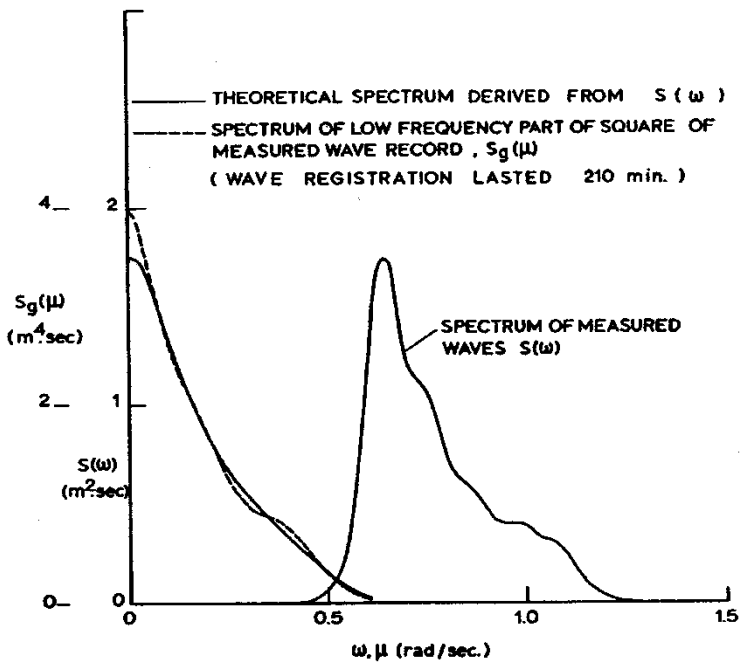

Figure A: Spectra of waves and low frequency part of the square of a wave record

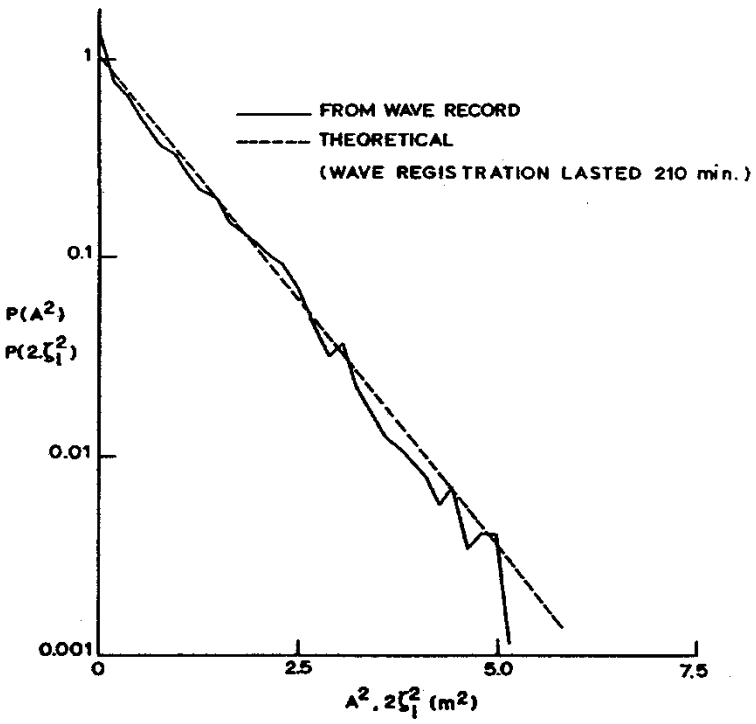

Figure B: Distribution function of the low frequency part of the square of a wave record

In order to show that this operation does indeed represent the wave envelope, results of an analyzed irregular wave train are plotted in the figure below showing the wave elevation ζ (t) and the corresponding wave envelope A (t).